Chapter 6

Isolation, characterization, *in vitro*, and *in vivo* investigation of hesperidin-loaded bovine milk exosomes

6 Isolation, characterization, *in vitro* and *in vivo* investigation of hesperidin-loaded bovine milk exosomes

6.1 Background

The study aimed to enhance the efficacy, anti-metastatic properties, and oral bioavailability of HES by loading it into bovine milk exosomes for melanoma treatment (Figure 6.1). Bovine milk-derived exosomes were prepared using the sonication method for HES loading. HES-loaded exosomes were characterized by particle size, morphology, encapsulation efficiency, X-ray diffraction, and drug release studies at pH 7.4 and pH 5.5. *In vitro* assays evaluated Exo-HES's anti-cancer activity, including cytotoxicity, cell uptake, ROS generation, mitochondrial membrane potential, and cell migration in B16F10 cells. Additionally, *in vivo* efficacy was tested using a B16F10-induced melanoma model, with toxicity assessed through histopathology and biochemical analysis.

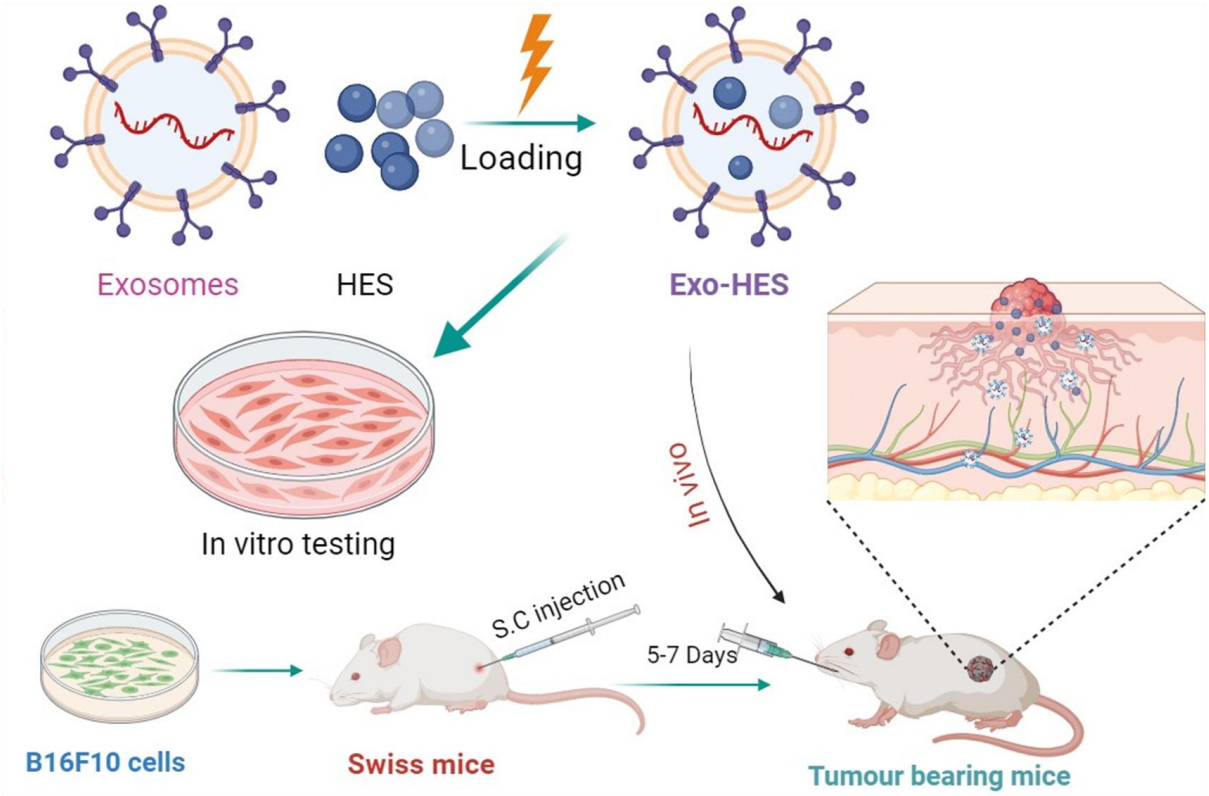

Figure 6.1 Graphical representation of the workflow for chapter 6.

6.2 Objectives

- Isolation of exosomes from bovine milk and HES loading via sonication method
- Pharmaceutical characterizations and stability studies of hesperidin-loaded (Exo-HES) exosomes
- *In vitro* anti-cancer efficacy and anti-migration studies
- *In vivo* oral bioavailability study
- *In vivo* anti-cancer efficacy study in melanoma (B16F10) bearing Swiss mice.

6.3 Methodology

6.3.1 HPLC analysis

6.3.1.1 *In vitro* analytical method

Method development

To determine the concentration of HES in exosomes, drug release studies, and other quantitative analyses, an HPLC method was developed and validated following ICH guidelines. The HPLC system used was an Agilent Infinity 1200 with a quaternary pump, autosampler, and Agilent 1200 PDA detector, controlled by Open LAB CDS EZChrom Workstation VL software.

Table 6.1 HPLC method parameters for HES

Parameters	Values
Mobile Phase	Methanol : water (80:20)
Column	RP- C18 (250 mm×4.6 mm. 5 µm; Thermo Scientific, USA)
Elution	Isocratic
Flow Rate	1 ml/min
Retention Time	3.6 min
Run Time	10 min
Column Temp.	25°C
λ_{max}	285 nm
Injection Volume	10 µl
Detector	PDA
LC Software	Open LAB CDS EZChrom Workstation VL software

A stock solution of HES (100 µg/ml) was prepared by dissolving 5 mg in 50 ml of methanol (HPLC grade) and diluted for working standards. Several mobile phase ratios (65:35, 68:32,

70:30, 80:20 v/v) of methanol and water were tested. The optimal retention time of 3.6 minutes was achieved using an 80:20 v/v methanol-water ratio. Chromatographic separation was performed with a reversed-phase C18 column (250 mm×4.6 mm, 5 μm; Thermo Scientific, USA) under the parameters listed in Table 6.1.

Method validation

The developed method was validated in accordance with ICH guidelines, evaluating parameters such as linearity, accuracy, precision, and specificity. The serial dilution technique was utilized to determine the LOD and LOQ (Guideline, 1997) [173].

Linearity

The linearity of the methods employed for HES analysis was assessed by constructing a standard curve correlating various analyte concentrations with the corresponding peak areas (detector responses). The concentration range was chosen based on expected drug concentrations in drug loading and drug release studies. Calibration curves consisting of eight points were generated over three consecutive days using standard working solutions. These solutions were injected in triplicate into the HPLC system. The linearity of the analytical methods was evaluated by plotting the peak area (detector response) against the analyte concentration. Linear regression analysis was performed to determine the slope, intercept, and the correlation coefficient (r^2).

Accuracy

Quality control (QC) samples at three distinct concentrations were analyzed to assess the accuracy of the analytical method for HES. The analysis was performed in triplicate (n = 3). The accuracy of the HPLC method was investigated from the percentage recovery by the standard addition method at three levels (50, 100, and 150%). Accurately 4, 8, and 12 μg/mL of working standard solution were added to pre-analyzed samples (8 μg/mL) to produce 6, 8,

and 10 µg/mL, respectively. The samples were analyzed by the developed HPLC method for quantifying the HES. The percent recovery was calculated by the equation below.

$$\% \text{ recovery} = \frac{Experimental\ or\ recovered\ concentration}{Theoretical\ concentration\ after\ addition} X\ 100$$

Precision

The precision (% RSD) of the method was evaluated by calculating the intra- and inter-day coefficient of variation. Intra-day precision was determined by analyzing three different concentrations of the drug in triplicate, conducted three times on the same day. Inter-day precision was evaluated by performing the same analysis on separate days, with the procedure repeated over three consecutive days.

Sensitivity (Detection and Quantitation limit)

The sensitivity of the analytical method is predicted by the LOD and LOQ. LOD is the lowest detectable concentration of the analyte while LOQ is the lowest amount of the analyte in a sample, which could be quantitatively determined with suitable precision and accuracy. LOQ was assessed by standard deviation of the response and the slope (S). Standard deviation was estimated by running the five blank samples while slope was determined based on calibration curve. LOD and LOQ for HES were determined following the guidelines of ICH (Guideline, 1997).

Robustness

The robustness of the developed HPLC method was studied by intentional changes in different chromatographic settings, such as wavelength (283, 285, and 287 nm), run times (8, 10, and 12 min), flow rate (0.8, 1, and 1.2 mL/min), mobile phase composition (78:22, 80:20, and 82:18 v/v of methanol:water), and analyzing the changes in the peak area and retention time (Rt) DHA of 12 µg/mL.

6.3.1.2 *In vivo* analytical method

The *in vivo* analytical method development and validation were carried out on the same HPLC system as employed during the analysis of the in vitro samples. The parameters for method development are given in the table below (Table 6.2).

Table 6.2 HPLC parameters for HES method development and validation for *in vivo* analysis

Parameters	**Values**
Mobile Phase	Methanol : water (80:20)
Column	RP- C18 (250 mm ×4.6 mm. 5 µm; Thermo Scientific, USA)
Elution	Isocratic
Flow Rate	1 ml/min
Retention Time	3.6 min
Run Time	10 min
Column Temp.	25°C
λ_{max}	285 nm
Injection Volume	10 µl
Detector	PDA
LC Software	Open LAB CDS EZChrom Workstation VL software

Sample preparation

Blood was collected from the retro-orbital plexus of female rats into the heparinized microcentrifuge tubes. Plasma was separated by centrifuging the blood at 10,000 rpm for 5 min at 4°C. Blank plasma (150 µl) was spiked with different concentrations of working standard solutions (50 µl) to give respective sets of calibration curve standards and QC samples. The plasma (50 µl) was mixed with 50 µl different concentrations of the HES (0.05 µg/ml to 25.6 µg/ml). A protein precipitating agent ACN (500 µl) was added and vortexed for 10 min. The mixture was centrifuged at 12,000 rpm for 10 min. After centrifugation supernatant was dried in vacuum drier at 40°C. The dried sample was reconstituted by adding 60 µl of mobile phase and transferred to auto-sampler vials, capped and placed in the HPLC autosampler. A 50 µl aliquot of each sample was injected into the HPLC column (system specifications are similar to the in vitro method).

Linearity and range

The linearity of the developed HPLC method was identified by observing the correlation coefficients obtained from the calibration curves of HES. The range of linearity was determined by fitting the data of average area (mAU) of three independent analyses with the corresponding concentration (µg/mL) to the linear equation and determining the concentrations range that follows the linearity.

Accuracy

Quality control (QC) samples at three distinct concentrations were analyzed to assess the accuracy of the analytical method for HES. The analysis was performed in triplicate (n = 3). The accuracy of the HPLC method was investigated from the percentage recovery by the standard addition method at three levels (50, 100, and 150%). Accurately 4, 8, and 12 µg/mL of working standard solution were added to pre-analyzed samples (8 µg/mL) to produce 6, 8, and 10 µg/mL, respectively. The samples were analyzed by the developed HPLC method for quantifying the HES. The percent recovery was calculated by the equation below.

$$\% \text{ recovery} = \frac{Experimental\ or\ recovered\ concentration}{Theoretical\ concentration\ after\ addition} X\ 100$$

Precision

The precision (% RSD) of the method was evaluated by calculating the intra- and inter-day coefficient of variation. Intra-day precision was determined by analyzing three different concentrations of the drug in triplicate, conducted three times on the same day. Inter-day precision was evaluated by performing the same analysis on separate days, with the procedure repeated over three consecutive days.

Sensitivity (Detection and Quantitation limit)

The sensitivity of the analytical method is predicted by the LOD and LOQ. LOD is the lowest detectable concentration of the analyte while LOQ is the lowest amount of the analyte in a sample, which could be quantitatively determined with suitable precision and accuracy. LOQ

was assessed by standard deviation of the response and the slope (S). Standard deviation was estimated by running the five blank samples while slope was determined based on calibration curve. LOD and LOQ for HES were determined following the guidelines of ICH (Guideline, 1997).

Robustness

The robustness of the developed HPLC method was studied by intentional changes in different chromatographic settings, such as wavelength (283, 285, and 287 nm), run times (8, 10, and 12 min), flow rate (0.8, 1, and 1.2 mL/min), mobile phase composition (78:22, 80:20, and 82:18 v/v of methanol:water), and analyzing the changes in the peak area and retention time (Rt) DHA of 12 µg/mL.

6.3.2 Isolation of exosomes

Exosomes were isolated from bovine milk through differential centrifugation [202]. Fresh milk was sourced from mid-aged cows in the mid-lactation period at a local dairy farm, BHU campus in Varanasi, India. The initial centrifugation was performed at 13,000 g for 30 minutes at 4°C (using a 32 Ti rotor on an Optima XPN-100 centrifuge, Beckman, MA, USA) to remove fat, cream, and proteins. After carefully discarding the fat layer, the milk was ultracentrifuged at 100,000 g for 60 minutes at 4°C to further eliminate proteins and dead cells. The resulting supernatant was collected and centrifuged at 130,000 g for 90 minutes at 4°C (32 Ti rotor, Optima XPN-100 centrifuge, Beckman, MA, USA). The exosomal pellets were then washed three times with chilled PBS, resuspended in PBS, quantified using the Bradford assay, and stored at -80°C until further use.

6.3.3 Drug loading

Sonication technique, as mentioned in chapter 5, was used to produce HES-loaded exosomes (Exo-HES). In brief, HES was dissolved in a mixture of ethanol and acetonitrile at a 1:1 ratio. Subsequently, the HES solution was combined with the exosomal solution at a ratio of 1:9 (1

mg of HES to 9 mg of exosomes with respect to protein content). The amalgam underwent six cycles of sonication at 20% amplitude (30 sec on, 30 sec off, and 2 min gap between cycles). The Exo-HES was sonicated and allowed to recover the exosomal membrane for an hour at room temperature. To determine the %DL and %EE, the HES was extracted and the exosomal protein was precipitated by adding methanol (0.7 ml) to Exo-HES (0.3 ml). The drug concentration was then assessed using HPLC, and %EE and %DL were calculated by using the following equation:

$$\textbf{Encapsulation efficiency (\%)} = \frac{\textit{Amount of drug encapsulated in exosomes}}{\textit{Total amount of drug added}} \textbf{X100}$$

$$\textbf{Drug loading (\%)} = \frac{\textit{Amount of drug encapsulated in exosomes}}{\textit{Total amount of drug and Exosomes in final formulation}} \textbf{X100}$$

6.3.4 Characterization

Using the DLS principle, the developed Exo and Exo-HES were evaluated for average particle size, PDI, and ZP using the DelsaNano particle analyzer (Beckman Coulter, CA, USA). AFM (INTEGRA Prima, NT-MDT Service & Logistics Ltd, Tempe, AZ, USA) and SEM were used to examine the morphology of Exo and Exo-HES. A small quantity (10 µl) of Exo and Exo-HES were diluted 600 times in fresh PBS followed by filtration through 0.22 m PVDF syringe filters. Filtered samples were placed on glass slides, dried off by air drying, then coated with gold, and examined by SEM. The same filtered samples were used for the AFM analysis. Samples (10 µl) were placed on clean silica glass and dried overnight. The height signal in the retrace direction and the cantilever's amplitude signal, both concurrently captured, were displayed in the trace direction to create images. The software program Nova Px 3.4.0 was then used to process the images.

6.3.5 X-Ray diffraction

The XRD patterns of Exo, HES, and Exo-HES samples were analyzed using a high-resolution XRD system (Rigaku Corporation, Tokyo, Japan) operating at 9 kW. The diffraction scans were

conducted over a 10–40° 2θ range with a scan rate of 10°/min [176]. For sample preparation, liquid samples were repeatedly applied onto small transparent glass slides to form a thin coating. Once the coating was achieved, the slides were mounted on a goniometer, and the DTEX detector was used to record the diffraction patterns [184].

6.3.6 Drug release studies

An *in vitro* drug release study, as outlined in section 5.3.8, was conducted to evaluate the release rate and extent of drug release at pH levels of 5.5 and 7.4. Dialysis bags (MWCO 14,000 Da, Himedia, Mumbai, India) were pre-treated by soaking in PBS overnight before the experiment. To maintain sink conditions, 50 ml of PBS of corresponding pH with 0.2% Tween 80 was added to the dialysis bags containing 1 mg each of HES and Exo-HES. The bags were then placed on a magnetic stirrer set to 37°C and 200 rpm. At predetermined intervals (0, 0.5, 1, 2, 4, 6, 8, 10, 12, 24, and 48 h), 3 ml samples were withdrawn and immediately replaced with fresh PBS. The collected samples were analyzed for drug concentrations using HPLC (Infinity 1200, Agilent Technologies, CA, USA).

6.3.7 Cells and culture conditions

HEK-293 cell lines were generously provided by Dr. Subash Chandra Gupta, Associate Professor, Department of Biochemistry, Institute of Science, Banaras Hindu University (BHU), Varanasi. B16F10 cell lines were procured from NCCS, Pune, Maharashtra, India. Both cell lines were grown in DMEM media (Himedia, India), supplemented with 10% fetal bovine serum (Gibco, Fisher Scientific, MA, USA), and 1% Antibiotic and Antimycotic solution (Himedia, Mumbai, India) containing 10,000 U Penicillin, 10 mg Streptomycin, and 25 µg Amphotericin B per ml. The cells were cultured in a humidified CO2 incubator (Heracell VIOS 160i, Thermo Fisher, MA, USA) at 37ºC.

6.3.8 Cell cytotoxicity and biocompatibility

The cytotoxicity and biocompatibility assessments of HES, exosomes, and Exo-HES were conducted in B16F10 and HEK-293 cell lines, respectively, utilizing the MTT assay. In brief, both cell lines were seeded in 96-well plates at a density of 5 X 10^3 cells/well and allowed to adhere overnight. Subsequently, the media were replaced with fresh media containing varying concentrations of HES, exosomes, and Exo-HES. For biocompatibility evaluation, the cells were incubated for 24 h, while for cytotoxicity assessment, the cells were incubated for 24, 48, and 72 h. After the respective incubation periods, the media was aspirated, 100 µl of MTT solution (5 mg/ml) was added to each well and further incubated for 4 h. Finally, 100 µl of DMSO was introduced to each well, and absorbance readings were taken at 590 nm (BioTek equipment located in Charlotte, Vermont, United States). The IC50 values were calculated utilizing GraphPad Prism software.

6.3.9 Qualitative cell uptake assay

To assess the internalization capacity of drug-loaded exosomes into cancer cells, a qualitative cell uptake experiment was conducted using coumarin-6 (C-6) loaded exosomes (Exo-C-6), following the method already described in section 5.3.11. Exo-C-6 was prepared in a manner similar to HES–Exo, with C-6 replacing HES. B16F10 cells were seeded in 6-well plates at a density of 5 x 10^4 cells/well and allowed to adhere overnight. Subsequently, the cells were incubated with Exo-C-6 (3 µg/ml) for 4 h. After the incubation period, the cells were washed three times with chilled PBS to remove excess Exo-C-6, and the internalized C-6 in cancer cells was visualized using fluorescence microscopy (Olympus BX53, Tokyo, Japan).

6.3.10 DNA-fragmentation assay with DAPI

The DNA-fragmentation assay was performed as described previously in section 5.3.12. Briefly, B16F10 cells were seeded at a density of 5 x 10^4 cells/dish in 35 mm Petri dishes (Tarsons, Kolkata, India) and incubated overnight for cell attachment. Subsequently, the cells

were treated with Exo, HES, and Exo-HES (equivalent to 18 µM of HES) and incubated for 24 h. After the incubation period, the media was removed, and cells were washed with cold PBS to eliminate any residual formulations. Following this, a 10-minute incubation period ensued with new media containing DAPI (5 µg/ml). After incubation, the medium was aspirated, cells were washed with fresh, ice-cold PBS, and examination was carried out using an Olympus BX53 fluorescent microscope (Tokyo, Japan).

6.3.11 Reactive oxygen species assay

To quantify the generation of intracellular ROS in cancer cells, the H2DCFDA dye was utilized. The cells were seeded in 35 mm petri dishes at a density of 5 x 10^4 cells/dish to allow attachment and were then incubated at 37°C overnight. Fresh media containing Exo, HES, and Exo-HES (equivalent to 18 µM of HES) were added, and the cells were incubated for an additional 24 h after the removal of the old media. Two hours before the completion of the treatment period, the cells were subjected to a 0.05% H_2O_2 treatment as a positive control. Following this treatment, 10 µM of H_2DCFDA was added to each petri dish and incubated for 30 minutes. Fluorescence was subsequently observed under a fluorescence microscope (Olympus BX53, Tokyo, Japan).

6.3.12 Mitochondrial membrane potential assay

Inhibition of MMP is one of the approaches by which HES impedes cancer progression. HES and Exo-HES's efficacy in suppressing MMP in B16F10 cell lines was examined using an MMP assay [203]. Briefly, 35 mm Petri dishes (Tarsons, Kolkata, India) were seeded with 5 x 10^4 B16F10 cells and then incubated overnight. Following the incubation, cells were washed and treated for 24 h with various formulations (Exo, HES, and Exo-HES, equivalent to 18 µM of HES). Following the completion of the treatment time, the media were withdrawn, fresh media were added with JC-1 dye (10 µg/ml), and further incubated for 30 minutes. The dye

was removed, and the cells were washed with fresh PBS before being examined under a fluorescence microscope (Olympus BX53, Tokyo, Japan).

6.3.13 Colony formation assay

A colony formation assay was conducted as outlined in section 5.4.13 to assess in vitro cell survival based on the ability of single cells to form colonies. Briefly, 100 cells were seeded into each 60 mm petri dish and allowed to adhere and grow overnight at 37°C. After 24 h of incubation, the medium was replaced with fresh medium containing Exo, HES, and Exo-HES (equivalent to 18 μM of HES). Media changes were then performed every other day for a total of ten days. On the final day, colonies were stained with 0.5% crystal violet and colony counts were manually recorded.

6.3.14 Wound healing assay

The wound healing assay for Exo, HES, and Exo-HES treatments was performed as previously described in section 5.3.18. In brief, B16F10 cells (5×10^4 cells/100 μl) were seeded in Culture-insert 2 well plates (Ibidi, Lochhamer Schlag, Gräfelfing, Germany) and incubated for 12 h to allow cell attachment. After attachment, the culture inserts were gently removed with sterile forceps to create a wound. Cells were then treated with Exo, HES, and Exo-HES (equivalent to 10 μM of HES, based on preliminary studies), rinsed with cold PBS, and incubated for 24 h. Wound healing was observed under an inverted microscope at 0, 12, and 24 h, and the percentage of wound closure was calculated using ImageJ software. The rate of wound closure was determined using the following formula:

$$\text{Rate of wound closure} = \frac{\textit{Distance wound closing } (\mu m)}{\textit{Time } (\textit{hours})}$$

Distance wound closing= Initial wound distance-final wound distance

6.3.15 Transwell migration assay

The cell migration assay aimed to assess the ability of the exosomal formulations to inhibit cell migration. B16F10 cells were pre-treated with exosomes, HES, and Exo-HES (equivalent to

10 µM of HES based on preliminary studies) for one hour before trypsinization and collection. A total of 0.5 ml of cells (4×10^2 cells/100 µL) were seeded in the upper chambers of six Transwell inserts (Sigma Aldrich, MA, USA) containing serum-free media, while media with 10% FBS was added to the lower chamber as a chemoattractant. After 24 h of incubation, the cells that migrated to the lower surface of the upper chamber were fixed with 4% formaldehyde and stained with 0.5% toluidine blue. Migrating cells were then counted using an inverted microscope (Dewinter, New Delhi, India).

6.3.16 Animal studies

All animal studies were approved by the Institutional Animal Ethics Committee (IIT(BHU)/IAEC/2024/I/003) and conducted in accordance with CPCSEA guidelines for animal care. Female Swiss albino mice, aged 8–10 weeks, were used for *in vivo* efficacy and metastasis studies. The animals were sourced from the Institute of Medical Science Animal House at Banaras Hindu University (BHU), Varanasi, India. They were housed under controlled conditions with a 12-hour light/dark cycle and provided with food and water ad libitum.

6.3.17 Pharmacokinetics

Female Sprague Dawley rats, aged 10–12 weeks, were divided into two groups (n=5 per group): Group I received HES, and Group II received Exo-HES. The animals were fasted for 12 hours before experimentation. Each group was administered a single oral dose of either Exo-HES (equivalent to 30 mg/kg HES) or HES (30 mg/kg, suspended in 0.5% carboxymethyl cellulose). Blood samples (200 µl) were collected from the retro-orbital vein under light anesthesia at predetermined time points (0.25, 0.5, 1, 2, 4, 6, 8, 10, 12, and 24 h post-administration). Samples were collected in heparinized tubes, centrifuged at 10,000 rpm for 10 minutes at 4°C to obtain plasma, and the drug was extracted with methanol. Plasma samples were then filtered through 0.22 µm nylon membrane filters (Merck, Bangalore, India) and

analyzed for drug concentration using HPLC (Infinity 1200, Agilent, USA). Pharmacokinetic parameters, including AUC, Tmax, Cmax, and elimination half-life, were calculated using PK Solver software.

6.3.18 *In vivo* anti-cancer efficacy

Swiss albino mice (aged eight weeks) were used to test the *in vivo* anticancer efficacy of various formulations and free drugs. Animals were acclimatized for one week with unrestricted access to food and water before the experiment. B16F10 cells were cultured in DMEM with 10% FBS until reaching 90% confluency, then harvested with trypsinization, adjusted to 5×10^5 cells/100 µl of media, and subcutaneously injected into the dorsal side of each mouse. Tumor size was measured every other day using digital vernier calipers. Once tumors reached 60–80 mm^3, mice were divided into groups (n=5 per group): Group I: Control (PBS); Group II: Exosomes (25 mg/kg, per oral); Group III: HES (30 mg/kg, per oral); Group IV: Exo-HES (equivalent to 30 mg/kg of HES, per oral); Group V: Dacarbazine (DTIC) at 5 mg/kg intraperitoneally. Healthy animals were also included to assess the toxicity profiles of the formulations and HES. Treatments were administered three times weekly over 20 days (a total of six doses), with tumor volume and body weight monitored on alternate days until the study's end. Blood was collected from the retro-orbital vein post-treatment to analyze biochemical parameters. After humane euthanasia by gentle cervical dislocation, vital organs (heart, liver, lungs, spleen, and kidneys) were collected for histopathological analysis, and tumors were excised for further examination.

6.3.19 Histopathology

Following the experiment, the tumor-bearing mice were sacrificed, and various organs, including the liver, lungs, heart, and spleen, were collected and preserved in a 10% formaldehyde solution. The organs were sectioned, embedded in paraffin wax, and sliced into thin sections (4–5 µm) using a cryotome (Leica, Germany). The sections were then stained with hematoxylin and eosin (H&E) to reveal histological changes post-treatment. Microscopic

examination and imaging of the slides were performed using a microscope (Dewinter, New Delhi, India).

6.3.20 Biochemical parameters

Following the completion of the *in vivo* efficacy experiment, biochemical and hematological parameters were assessed for toxicity evaluation. Blood (150 µl) was collected from the retro-orbital plexus into heparinized 1 ml centrifuge tubes before the sacrifice of the animals. Hematological parameters, including white blood cells, red blood cells, and platelets, were analyzed using an automated hematology analyzer (Microbion, Life Sciences, New Delhi, India). Serum samples were obtained for biochemical parameter analysis. Various biochemical parameters, including ALT, AST, ALP, urea, and creatinine, were measured using ELISA kits (ARKAY Healthcare Pvt. Ltd., Gujarat, India) with a biochemical analyzer (CHEM-5-Plus v2, Erba Mannheim, Germany).

6.3.21 Statistical analysis

The data was analyzed using the GraphPad Prism statistical program (Version 8.0; San Diego. CA, USA) and ImageJ software (Bethesda, Maryland, USA). To find out if there are any statistically significant differences between the means of three different experiments, analysis of variance (ANOVA) was employed. Statistics were deemed significant at p-values less than 0.05.

6.4 Results and discussion

6.4.1 HPLC Analysis

6.4.1.1 In vitro analytical method

The in vitro analytical HPLC method was developed for HES to calculate the HES concentration in the test samples while performing studies like drug loading, encapsulation efficiency determination, and *in vitro* drug release (Figure 6.2).

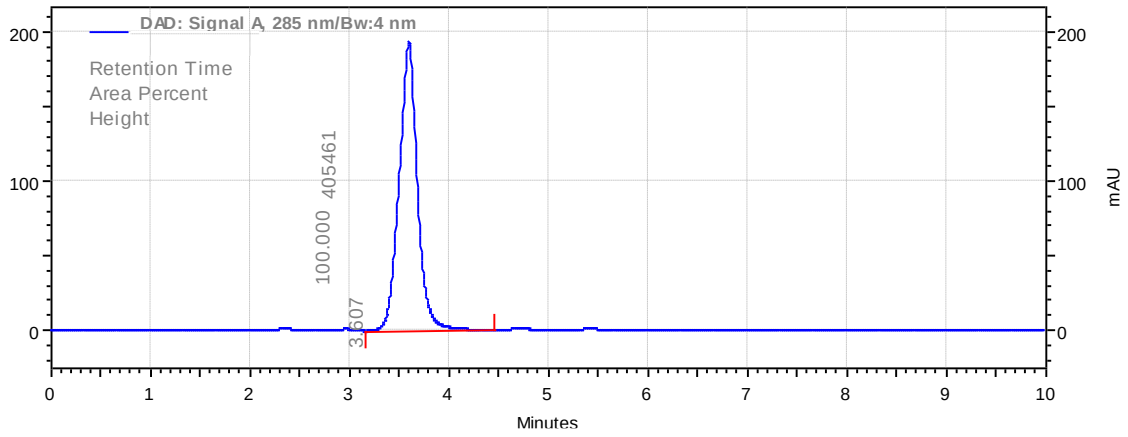

Figure 6.2 The HPLC and DAD signal chromatograms of HES at wavelength 285 nm, mobile phase methanol: water (80:20).

Linearity and range

Figure 6.3 shows the average area of the triplicate measurements for HES plotted against the corresponding concentrations. The selected HES concentrations range from 2 µg/mL to 20 µg/mL, and the Lambda max area (at 285 nm) demonstrated a linear relationship, with a correlation coefficient of $r^2 = 0.9962$ and a regression equation of $y = 92185x - 36763$.

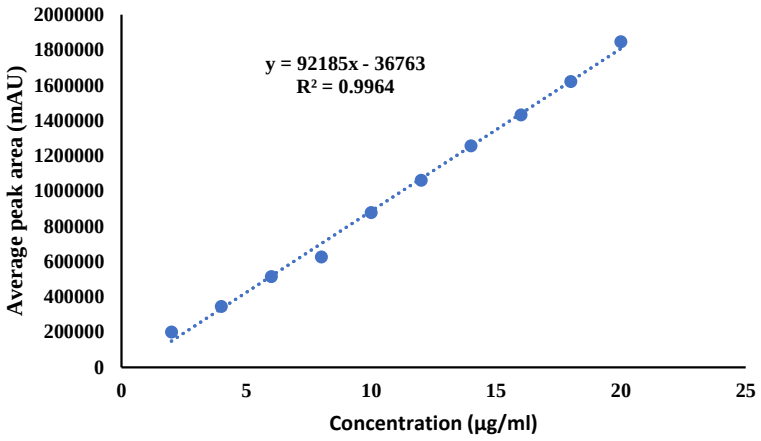

Concentration (µg/ml)	Average peak area (mAU)
2	198904
4	343534
6	513816
8	625658
10	877088
12	1060213
14	1256061
16	1431368
18	1620579
20	1845548

Figure 6.3 HPLC-based calibration curve of HES measured at 285 nm.

Accuracy

The accuracy of an analytical method can be determined by closely comparing its theoretical and experimental values. Table 6.3 presents the HES accuracy results as a percentage of recovery and percentage of relative standard deviation (% RSD). The enhanced HPLC method

demonstrates exceptional accuracy, as indicated by its high recovery values and low % RSD (<2%).

Table 6.3 Accuracy studies of the developed HPLC method for HES (n=3)

Concentration of HES (µg/ml)	Level (%)	HES Spiked concentration (µg/ml)	Theoretical concentration (µg/ml)	Experimental concentration (µg/ml)	% Recovery	% RSD
5	50	2.5	7.5	7.472±0.042	99.63	0.742
5	100	5	10	9.970±0.124	99.7	0.985
5	150	7.5	12.5	12.706±0.131	101.64	1.121

Precision

Precision, defined as the closeness of agreement among readings taken from multiple specimens of the same homogeneous sample under specified analytical conditions, was evaluated in this study. Repeatability and intermediate precision (intra-day and inter-day) experiments were conducted to assess the precision of the HPLC method at different concentrations of the working standard solution (6, 10, and 14 µg/mL). For HES, the percentage RSD value from the repeatability analysis was determined to be 0.09% (Table 6.4).

Table 6.4 Repeatability study of HES-developed HPLC method (n=8)

Concentration of HES (µg/ml)	Mean peak area	SD	RSD (%)
10	876384.7	830.49	0.094

Table 6.5 Intermediate precision (Intra-day and inter-day precision) studies of the HES-developed HPLC method

Concentration of HES (µg/ml)	Intra-day (at an interval of 6h)	RSD (%)	Inter (Day 1- Day 3)	RSD (%)
	Obtained Avg. peak area± SD (mAU)		Obtained Avg. peak area± SD (mAU)	
6	504570±3466.75	0.687	508018.66±1543.35	0.303
10	874154.66±8418.05	0.962	875133±4136.11	0.472
14	1241761±1848.36	0.148	1251713.33±12512.31	0.999

Table 6.5 summarizes the results of the intermediate precision studies. The percentage RSD values for the HES peak area in intra-day precision studies ranged from 0.148 to 0.962%, while

the inter-day precision studies showed percentage RSD values from 0.303 to 0.999%. All percentage RSD readings remained below 2%, meeting regulatory requirements and demonstrating the high precision of the developed HPLC method.

LOD and LOQ

The LOD and LOQ values for HES determination were found to be 0.242 and 0.689 µg/mL, respectively. The HPLC method's sensitivity for HES analysis was demonstrated by the reduced LOD and LOQ values.

Robustness and Ruggedness

Robustness measures the HPLC technique's resistance to small, deliberate changes in method variables, indicating its reliability under typical operating conditions.

Table 6.6 Robustness and ruggedness study of developed HPLC method for HES (10 µg/ml)

Parameters	Variations made	Area± SD (mAU)	RSD (%)	Retention time (RT)±SD (min)	RSD (%)
Wavelength	283	843594.333±1491.938	0.158	3.494±0.018	0.822
	285	877088.667±1176.438	0.134	3.698±0.06	0.287
	287	884676.384±848.613	0.089	3.842±0.021	0.95
Run time (min)	8	872963.666±5390.644	0.617	3.581±0.031	0.754
	10	879297.254±1153.323	0.142	3.631±0.021	0.854
	12	877963.451±10214.811	1.063	3.596±0.0189	0.962
Flow rate (mL/min)	0.8	918182±1248.705	0.135	3.495±0.022	0.955
	1	869021±1362.605	0.235	3.598±0.052	0.855
	1.2	922190±4562.635	0.505	3.587±0.006	0.252
Mobile phase composition (Methanol: Water)	78:22	883237.667±8115.468	0.918	3.382±0.025	1.122
	80:20	868012.258±0.542	0.875	3.612±0.024	0.798
	82:18	890149±9846.311	1.106	3.365±0.016	0.725

The robustness and ruggedness of the established HPLC method were evaluated through intentional modifications across various chromatographic settings. The results showed reduced percentage RSD values (<2%) for both area and retention time (Table 6.6), confirming the method's robustness.

6.4.1.2 *In vivo* analytical method

The HPLC method for HES was developed in plasma to calculate the HES concentration in the test samples while performing pharmacokinetic and drug distribution studies. The HES retention time was found at 3.6 min (Figure 6.4 A), while no drug peak was observed blank plasma (Figure 6.4 B)

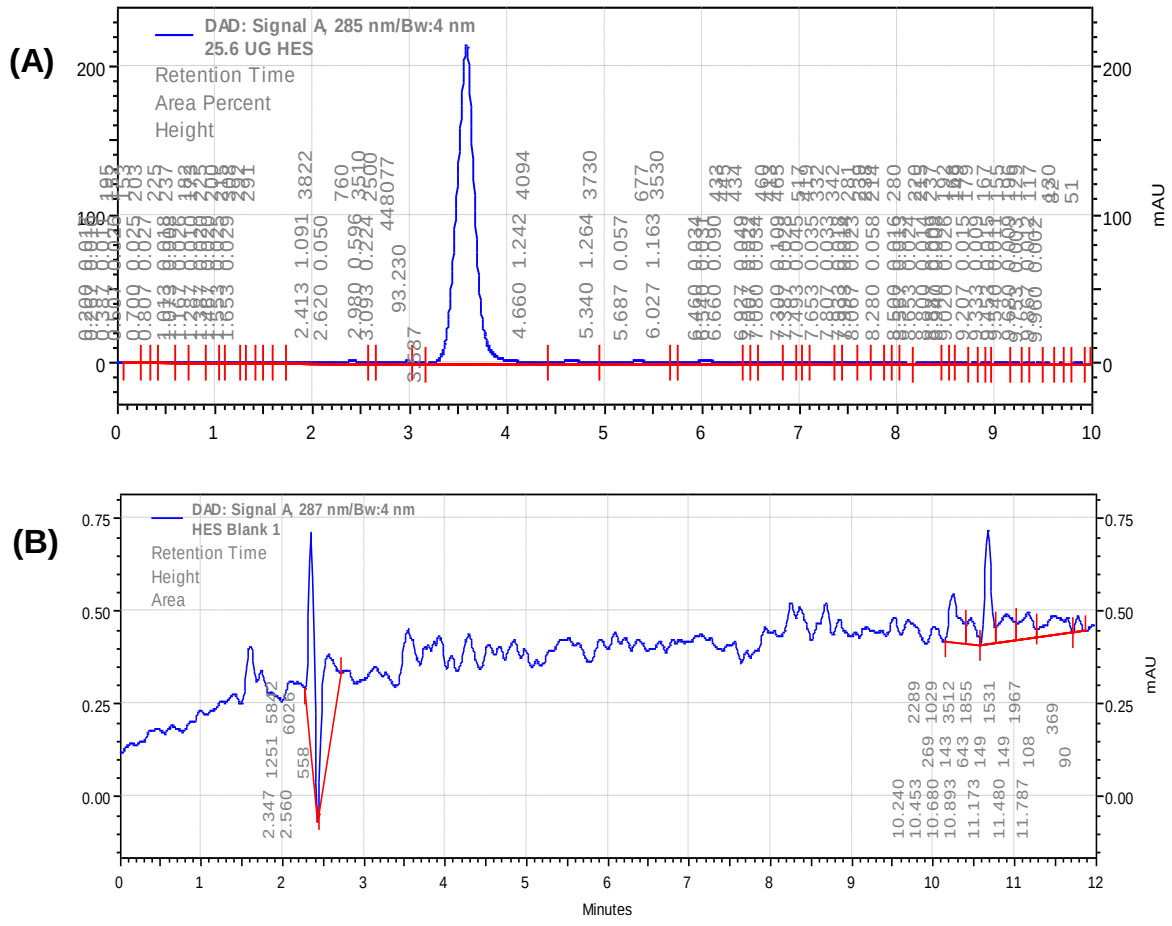

Figure 6.4 (A) HPLC and DAD signal chromatograms of HES in plasma and (B) blank plasma at wavelength 266 nm, mobile phase methanol: water (80:20).

Linearity and range

Figure 6.5 shows the average area of the triplicate measurements for HES plotted against the corresponding concentrations. The selected HES concentrations range from 0.05 µg/mL to 25.6 µg/mL, and the Lambda max area (at 285 nm) displayed a linear relationship, with a correlation coefficient of $r^2 = 0.9971$ and a regression equation of y = 31836x - 6174.5.

Concentration (µg/ml)	Area
0.05	82201
0.1	99054
0.2	105123
0.4	112120
0.8	132512
1.6	162521
3.2	205462
6.4	325461
12.6	529676
25.2	897258

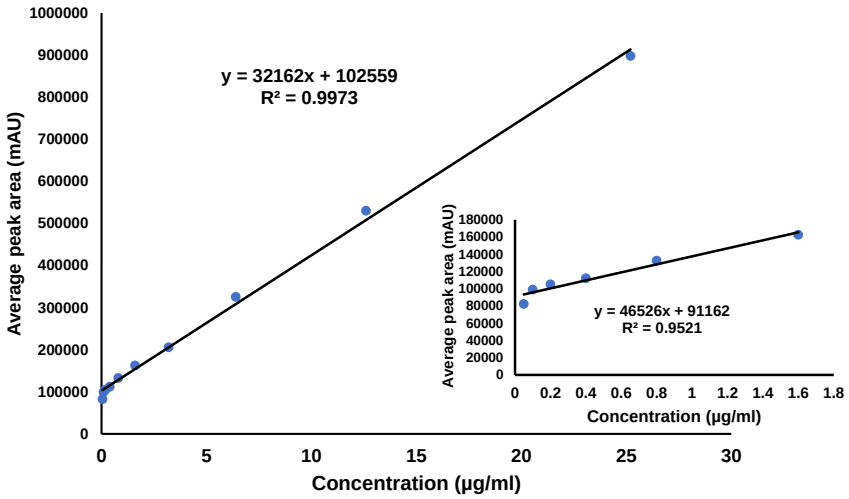

Figure 6.5 HPLC-based calibration curve of HES in plasma measured at 285 nm.

Accuracy

The accuracy of an analytical method can be determined by closely comparing its theoretical and experimental values. Table 6.7 presents the HES accuracy results as a percentage of recovery and percentage of relative standard deviation (% RSD). The enhanced HPLC method demonstrates exceptional accuracy, as indicated by its high recovery values and low % RSD (<2%).

Table 6.7 Accuracy studies of the developed HPLC method for HES (n=3)

Concentration of HES (µg/ml)	Level (%)	HES Spiked concentration (µg/ml)	Theoretical concentration (µg/ml)	Experimental concentration (µg/ml)	% Recovery	% RSD
5	50	2.5	7.5	7.389±0.042	99.63	0.568
5	100	5	10	9.890±0.124	99.52	1.253
5	150	7.5	12.5	12.526±0.131	101.64	1.045

Precision

Precision, defined as the closeness of agreement among readings taken from multiple specimens of the same homogeneous sample under specified analytical conditions, was evaluated in this study. Repeatability and intermediate precision (intra-day and inter-day) experiments were conducted to assess the precision of the HPLC method at different concentrations of the working standard solution (6, 10, and 14 µg/mL). For HES, the percentage RSD value from the repeatability analysis was determined to be 0.09% (Table 6.8).

Table 6.9 summarizes the results of the intermediate precision studies. The percentage RSD values for the HES peak area in intra-day precision studies ranged from 0.148 to 0.962%, while the inter-day precision studies showed percentage RSD values from 0.303 to 0.999%. All percentage RSD readings remained below 2%, meeting regulatory requirements and demonstrating the high precision of the developed HPLC method.

Table 6.8 Repeatability study of HES-developed HPLC method (n=8)

Concentration of HES (µg/ml)	Mean peak area	SD	RSD (%)
10	866284.7	2859.49	0.330

Table 6.9 Intermediate precision (Intra-day and inter-day precision) studies of the HES-developed HPLC method

Concentration of HES (µg/ml)	Intra-day (at an interval of 6h)	RSD (%)	Inter (Day 1- Day 3)	RSD (%)
	Obtained Avg. peak area± SD (mAU)		Obtained Avg. peak area± SD (mAU)	
6	524570.58±3466.75	0.660	518018.66±1943.35	0.375
10	884154.66±7418.05	0.838	845133.54±3936.11	0.472
14	1141761±3848.36	0.337	1351713.33±12512.31	0.925

LOD and LOQ

The LOD and LOQ values for HES determination were found to be 0.242 and 0.689 µg/mL, respectively. The HPLC method's sensitivity for HES analysis was demonstrated by the reduced LOD and LOQ values.

Robustness and Ruggedness

Robustness measures the HPLC technique's resistance to small, deliberate changes in method variables, indicating its reliability under typical operating conditions. The robustness and ruggedness of the established HPLC method were evaluated through intentional modifications across various chromatographic settings. The results showed reduced percentage RSD values (<2%) for both area and retention time (Table 6.10), confirming the method's robustness.

Table 6.10 Robustness and ruggedness study of developed HPLC method for HES (10 µg/ml)

Parameters	Variations made	Area± SD (mAU)	RSD (%)	Retention time (RT)±SD (min)	RSD (%)
Wavelength	283	833594.373±3491.938	0.418	3.564±0.018	0.822
	285	867088.617±2176.438	0.250	3.688±0.064	0.287
	287	894676.434±3128.613	0.349	3.852±0.021	0.955
Run time (min)	8	878963.766±5390.644	0.613	3.561±0.031	0.754
	10	877297.824±3153.323	0.359	3.641±0.021	0.854
	12	873963.445±2014.811	0.230	3.598±0.018	0.962
Flow rate (mL/min)	0.8	928718.554±3248.705	0.349	3.475±0.022	0.955
	1	869021.965±3362.605	0.386	3.568±0.052	0.855
	1.2	922190.655±4562.635	0.494	3.587±0.016	0.252
Mobile phase composition (Methanol: Water)	78:22	883237.667±8115.468	0.918	3.382±0.025	1.122
	80:20	868012.258±5120.542	0.589	3.712±0.024	0.798
	82:18	890149.514±9846.311	1.106	3.565±0.016	0.725

6.4.2 Isolation and characterization of bovine milk exosomes and hesperidin-loaded exosomes

The average size, PDI, and zeta potential of bovine milk exosomes were 92.8±4.1nm, 0.107±0.005, and -23.2±1.8 mV, respectively. For the Exo-HES, these values were 106.7±3.1nm, 0.129±0.003, and -27.6±1.9 mV, respectively (Figure 6.6 A-G, and Table 6.7). The difference in particle size indicates that the HES is actively loaded into the Exo; yet, the difference in size was not significant, and the findings are consistent with previous studies

[204]. Exo-HES was shown to have a greater negative zeta potential (-27.6±1.9) than naïve exosomes (-23.2±1.8), suggesting that both Exo and Exo-HES were stable. The binding or attachment of some of the HES's functional groups to the exosomal surface by hydrogen bonding or basic ionic interactions is responsible for the changes in the zeta potential.

Formulation	Size (nm)	PDI	Zeta potential (ζ)	EE%	DL%
Exo	92.8±4.1	0.107±0.005	-23.2±1.8	-	-
Exo-HES	106.7±3.1	0.129±0.003	-27.6±1.9	79.9±2.5	18.5±1.4

Table 6.11 Particle size, PDI, zeta potential, encapsulation efficiency, and drug loading of exosomes and HES-loaded exosomes

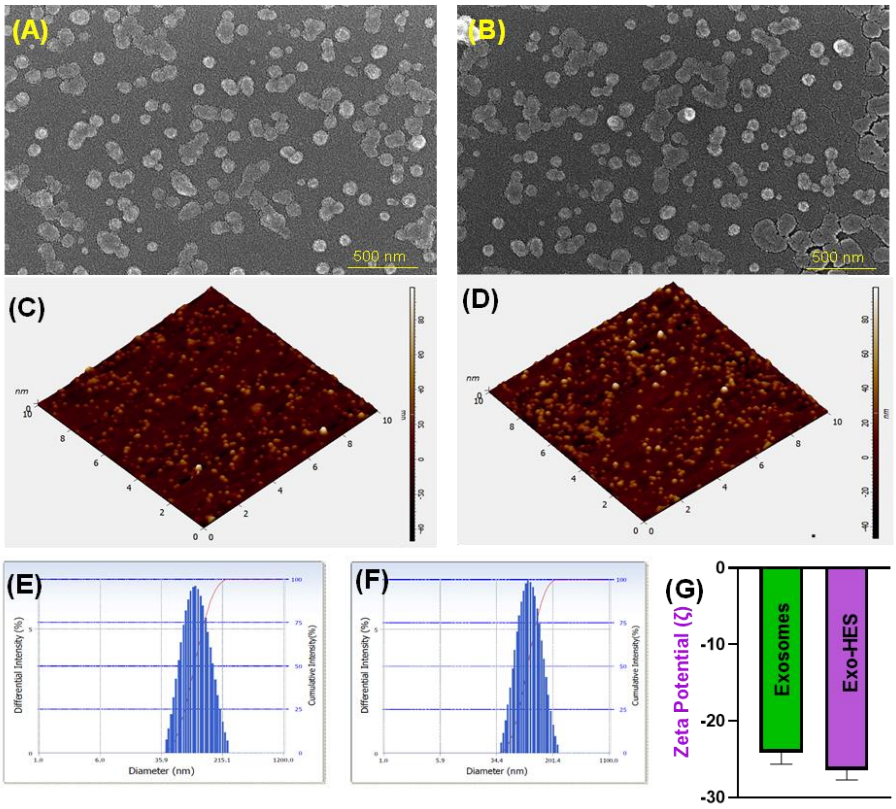

Figure 6.6 Morphology of exosomes and Exo-HES: (A-B) Morphology by SEM, (C-D) morphology by AFM of Exo and Exo-HES, (E-F) size of Exo and Exo-HES via particle size analyzer, and (G) zeta potential.

It was also found that the percentages of drug loading and encapsulation efficiency were 18.6±1.4 and 79.9±2.5, respectively. SEM and AFM were used to visualize the surface

morphology of Exo and Exo-HES (Figure 6.6 A-B, C-D). Exo and Exo-HES are both spherical, according to their morphology, and the size determined by electron microscopy was around 80 nm smaller than the size determined by the particle size analyzer. Because the particle size analyzer analyses

the hydrodynamic size, a variation in the size measurement was observed. On the other hand, the SEM and AFM measure the single entity's true size [205]. Furthermore, the exosomes' structure did not alter even after HES was loaded, suggesting that exosomes constitute an appropriate delivery system for HES.

6.4.3 X-ray diffraction

Exo, HES, and Exo-HES X-ray diffraction patterns were examined. In the case of exosomes, depicted in Figure 6.7 (A), a singular peak is evident at 32.63º, signifying the crystalline structure of the exosomes. HES displays several distinct peaks at 12.56°, 13.81°, 16.34°, 16.48°, 18.24°, 19.69°, 21.23º, 22.64º, 24.25º, and 25.01º, indicating its crystalline nature.

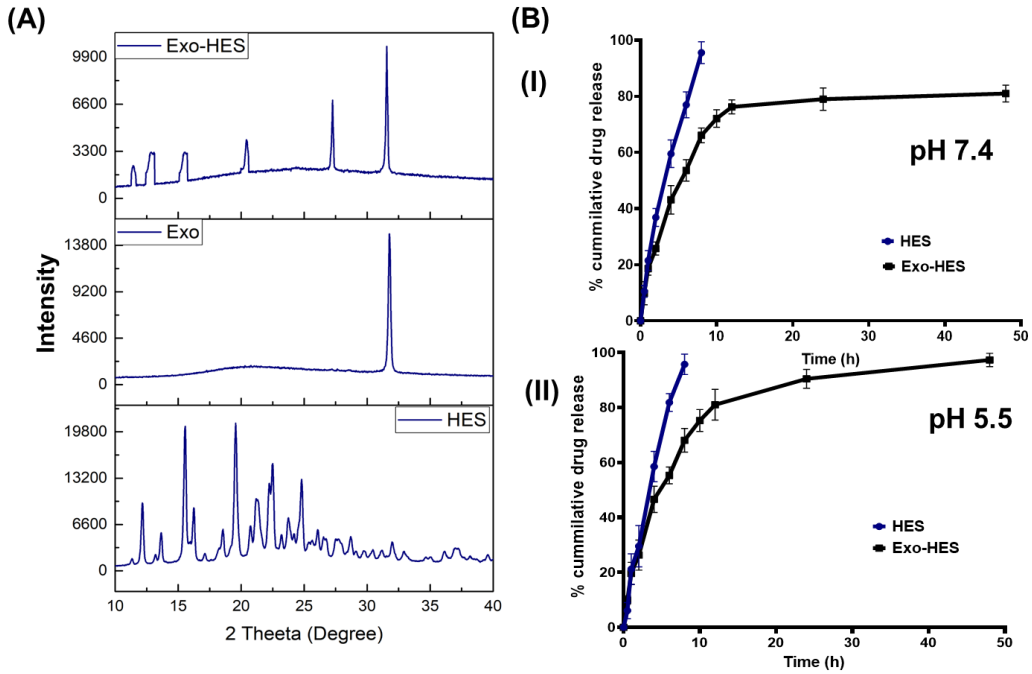

Figure 6.7 XRD and drug release profile of exosomes, HES, and Exo-HES. (A) Represents XRD of exosomes, HES, Exo-HES, (B) Drug release profile at (I) pH 7.4 and (II) pH 5.5.

The distinctive peaks of Exo and HES in the case of Exo-HES are observed at 13.26°, 17.15°, 21.45°, 27.55º, and 33.4º. Notably, Exo-HES does not manifest all the distinctive HES peaks, and several peaks are weakly represented with slight variations in theta values. It is hypothesized that the binding of HES to the exosomal surface through hydrophobic contact and variations in their binding energy contribute to the minor changes in 2 theta and the disappearance of specific peaks [202, 206].

6.4.4 Drug release

The *in vitro* release profiles of HES and Exo-HES were evaluated under two distinct pH environments: pH 5.5, representing the tumor microenvironment, and pH 7.4, simulating blood conditions. Figure 6.7 B (I&II) illustrates the biphasic release profile of HES from Exo-HES, while HES exhibited a continuous release, releasing the entire drug within 8 hours under both pH conditions. In the initial two hours of the Exo-HES experiment at both pH environments, approximately 20% of HES was released from exosomes, followed by sustained release up to 48 h. This sustained release accounted for 82% of HES release at pH 7.4 and 98% at pH 5.5. The burst release may result from HES partially attaching to the exosome surface through hydrophobic interactions or forming hydrogen bonds [202]. Conversely, the prolonged release is attributed to the diffusion of HES trapped inside the exosomes [206]. The distinct release pattern of HES from exosomes suggests its potential utility in both short- and long-term therapeutic strategies for inhibiting tumor growth. Moreover, the pH of 5.5, representative of the acidic tumor microenvironment, may induce the rupture of the exosomal membrane, facilitated by proteins and peptidoglycans, leading to increased drug release [207, 208]. This implies higher drug release at pH 5.5.

6.4.5 Cytotoxicity

The cytotoxicity assessment serves as a standard method to evaluate the anti-cancer properties of newly identified compounds. In this study, B16F10 and HEK-293 cell lines were employed

to investigate the cytotoxicity and safety of HES. The MTT assay, which relies on the conversion of MTT into insoluble purple formazan crystals by viable cells, was utilized. Lack of crystal formation indicates cell death, establishing a direct correlation between cell survival and color production. The experiment spanned 24, 48, and 72 h, as depicted in Figure 6.8 (A-D). After a 24 h treatment, the calculated IC50 values for HES and Exo-HES were found to be 17.50±1.02 and 14.02±1.12 µM, respectively. Substantial reduction in IC50 values occurred at 48 h, with HES and Exo-HES showing IC50 values of 13.25±0.90 and 10.20±1.10 µM, respectively. This trend persisted after a 72 h treatment. The observed decrease in IC50 values for HES and Exo-HES suggests enhanced internalization of HES into cancer cells facilitated by exosome delivery. Additionally, the safety of HES and Exo-HES was evaluated in HEK-293 cell lines. Even at a dosage of 60 µM of HES, no detectable cytotoxicity was observed (Figure 6.8 (E).

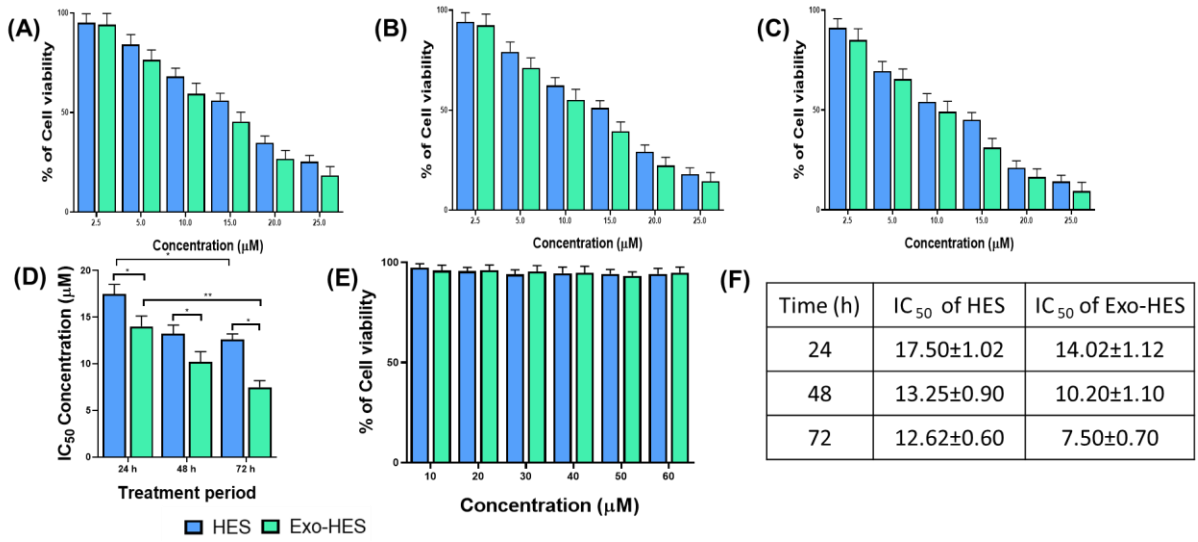

Time (h)	IC_{50} of HES	IC_{50} of Exo-HES
24	17.50±1.02	14.02±1.12
48	13.25±0.90	10.20±1.10
72	12.62±0.60	7.50±0.70

Figure 6.8 Cytotoxicity of HES and Exo-HES at different time points: (A) 24 h, (B) 48 h, (C) 72 h., and (D) IC50 values at different time points. Additionally, (E) depicts cell viability in HEK-293 cell lines, and (F) represents the IC50 values in tabular form. Statistical analysis was conducted using One-Way ANOVA, followed by the Tukey post hoc test for multiple comparisons. The significance levels are denoted as *$p < 0.05$, **$p < 0.01$.

This lack of cytotoxicity towards normal cells is commonly observed due to the rapid division of cancer cells, making them more susceptible to anti-cancer drugs compared to healthy cells. Additionally, cancer cells often exhibit reduced abilities to detect and repair DNA damage,

increasing the likelihood of ineffective DNA replication and eventual apoptosis or mitotic catastrophe [209]. Thus, it was concluded that HES and Exo-HES do not exhibit harmful effects on normal cell lines.

6.4.6 Qualitative cell uptake assay

An intracellular uptake experiment was conducted to validate the ability of exosomes to be internalized into cancer cells. As HES lacks fluorescence, coumarin-6 (C-6) was used as a surrogate, incorporated into exosomes (Exo-C-6) to assess intracellular uptake. The lipophilic dye C-6 mimic the HES for characteristics. Figure 6.9 demonstrates that the green fluorescence of Exo-C-6 is remarkably higher than that of free C-6. In contrast, the untreated C-6 group displayed no green fluorescence, indicating that the observed fluorescence results from C-6 uptake. Moreover, the nucleus was stained with DAPI to further confirm the uptake of exosomes inside the cell or attached to the surface.

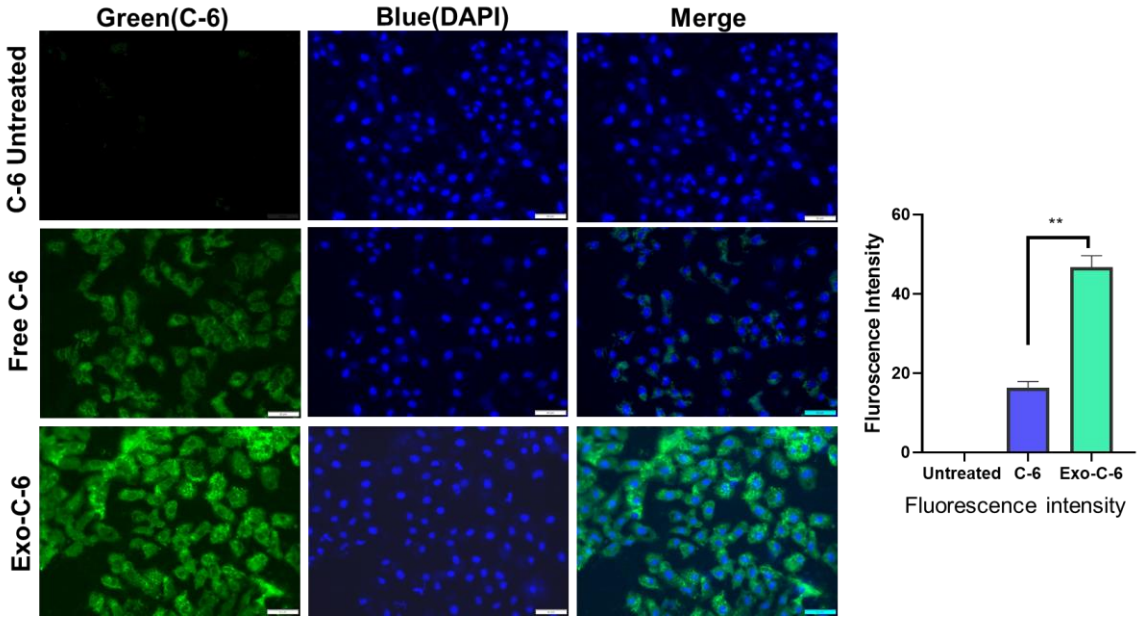

Figure 6.9 Qualitative cellular uptake of free coumarin-6 and coumarin-6 loaded exosomes in B16F10. Cells were observed in brightfield, the green channel for C-6, and the blue channel for DAPI.

The findings indicated that C-6 was internalized by the cells, validating the intracellular uptake of exosomes. Furthermore, a separate investigation was done previously [210] using PKH-67 labeled bovine milk exosomes to explore the uptake mechanism in H1299 cell lines. The results

demonstrated that exosome cellular uptake relies on energy, as evidenced by pre-treatment with 0.1% sodium azide inhibiting uptake. Additionally, the pathway of cellular uptake was identified as involving caveolin-1 and clathrin-mediated processes.

6.4.7 DNA-Fragmentation assay

HES induces apoptosis in cancer cells through both intrinsic (via the external death receptor) and extrinsic (by the nucleus) pathways. The nuclear fragmentation assay labeled the nuclei with DAPI to assess the intrinsic apoptosis pathway. Morphological changes were observed, including condensed or fragmented nuclei and horseshoe-shaped nuclei. Figure 6.10 illustrates the altered shape of nuclei treated with Exo-HES, displaying a fragmented and disoriented structure compared to the control and HES groups.

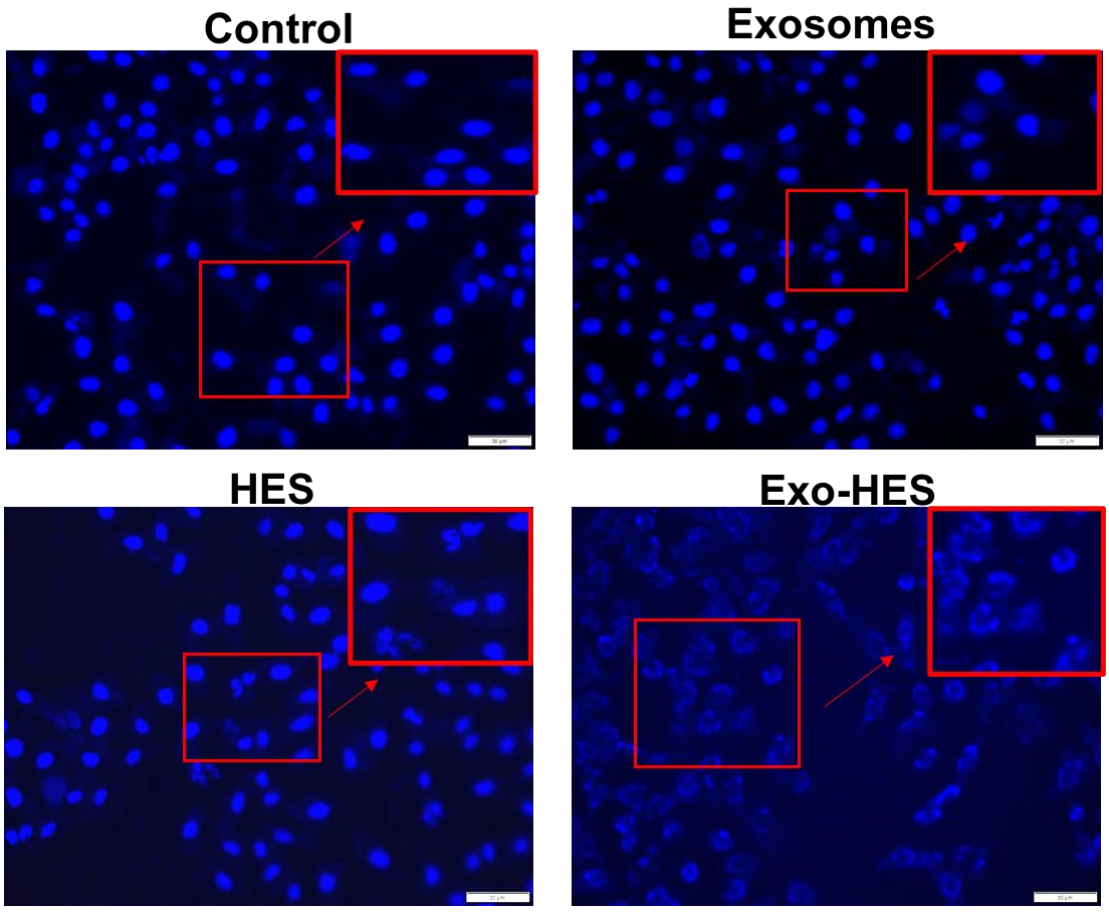

Figure 6.10 Nuclear DNA fragmentation assay performed with DAPI staining.

The alterations in nuclear morphology are commonly linked to the activation of apoptotic regulators like BCL-2 and survivin or as a response to DNA damage. The balance between apoptotic and anti-apoptotic factors plays a vital role in cellular homeostasis. Based on the DNA fragmentation assay findings, we hypothesize that HES impedes cell proliferation by upregulating apoptotic factors and inducing DNA damage. Furthermore, the increase in apoptotic factors and decrease in anti-apoptotic factors due to DNA damage by HES aligns with the previous findings [213] indicating that HES triggers apoptosis through an intrinsic mechanism [154].

6.4.8 Reactive oxygen species assay

Reactive oxygen species production by cells plays a crucial role in apoptosis and cellular damage, with elevated ROS levels being a common biochemical feature in inhibiting the development of cancer cells and altering redox states. The administration of chemotherapy drugs often triggers a significant rise in ROS levels within cells. Oxidative stress is a prominent factor in the early stages and progression of various cancer types, including melanoma.

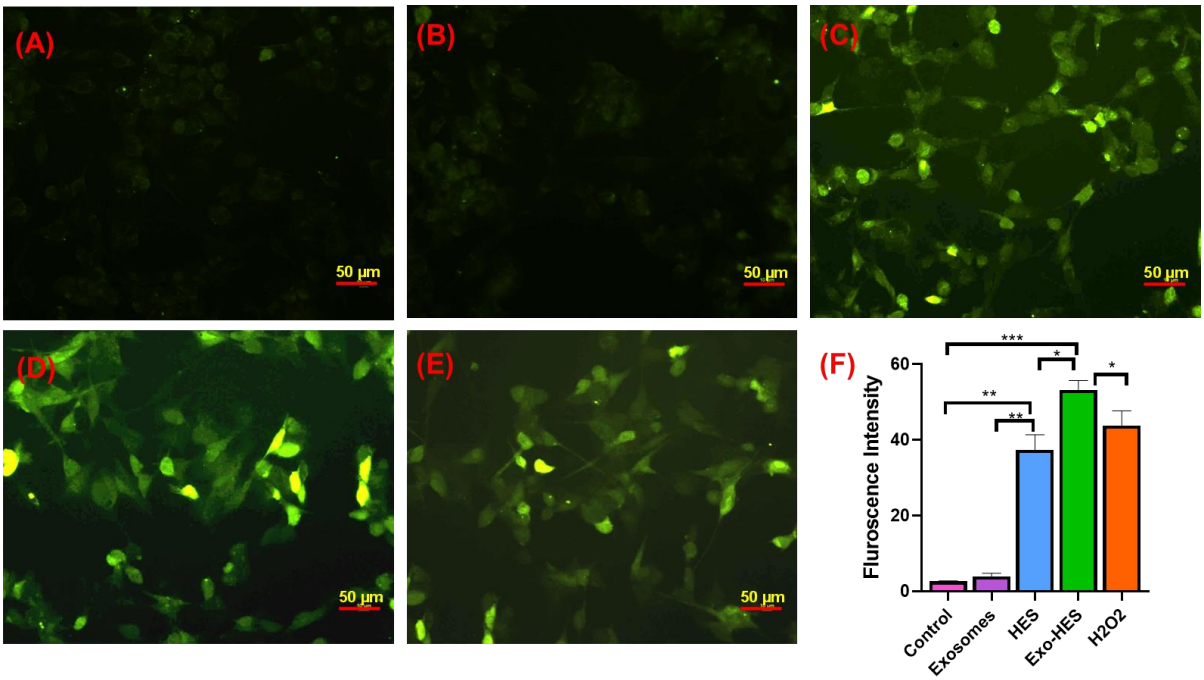

Figure 6.11 The generation of reactive oxygen species was estimated via H2DCFDA dye. (A) represents no treatment, (B) exosomes treated, (C) HES treated, (D) Exo-HES treated. (E)

H2O2, (F) Fluorescence intensity. Statistical analysis was performed by One-Way ANOVA followed by the Tukey P test with multiple comparisons and the significance level *$p < 0.05$, **$p < 0.01$, and ***$p < 0.001$.

Evidence from epidemiological, clinical, and experimental studies suggests that oxidative cell damage is closely linked to melanoma development. In our study, we utilized H2DCFDA dye to validate the induction of ROS and oxidative stress by HES. Results showed that treatment with Exo-HES significantly increased the fluorescence intensity of cells compared to HES treatment ($p<0.05$), as depicted in Figure 6.11. Untreated cells served as the negative control, while cells treated with H2O2 were the positive control in terms of ROS generation and oxidative stress. Despite the generation of a small amount of ROS, the level is sufficient to exceed the threshold to induce oxidative stress to an even greater extent, leading to apoptosis. Our results are supported by previously published data [211].

6.4.9 Mitochondrial membrane potential assay

Mitochondria, often referred to as the "powerhouse" of cells, play a crucial role in indicating the health status of a cell. Early stages of apoptosis, or cell death, are characterized by the loss of mitochondrial membrane potential, allowing mitochondrial contents to leak into the cell's cytoplasm. The dye JC-1, which is membrane-permeant and cationic, is commonly used to monitor mitochondrial health. In healthy cells, a high concentration of JC-1 accumulates inside the mitochondria due to the membrane potential, emitting red fluorescence. However, during apoptosis, disrupted membrane potential leads to JC-1 dissociation and the emission of green fluorescence [212]. Based on our experimental findings, we can differentiate between the intrinsic mitochondrial apoptosis pathway and the receptor-mediated extrinsic apoptosis pathway by detecting initiator caspase-8 or -9, respectively [213]. Activation of either pathway leads to the activation of common executor caspases (caspase-3 and caspase-7), initiating apoptosis. In our study, we assessed mitochondrial membrane potential (MMP) using JC-1 dye, and Figure 6.12 illustrates a significant reduction in JC-1 aggregate production in Exo-HES

compared to HES, as indicated by fluorescence intensity ($p<0.05$). These results align with previous research, showing that HES inhibits cell growth by downregulating apoptotic proteins such as BCl-2 and upregulating anti-apoptotic proteins such as cytochrome C, cleaved caspase 3, cleaved caspase 9, and BAX [214]. The overall apoptotic results suggest that HES functions against cancer by decreasing the mitochondrial membrane potential.

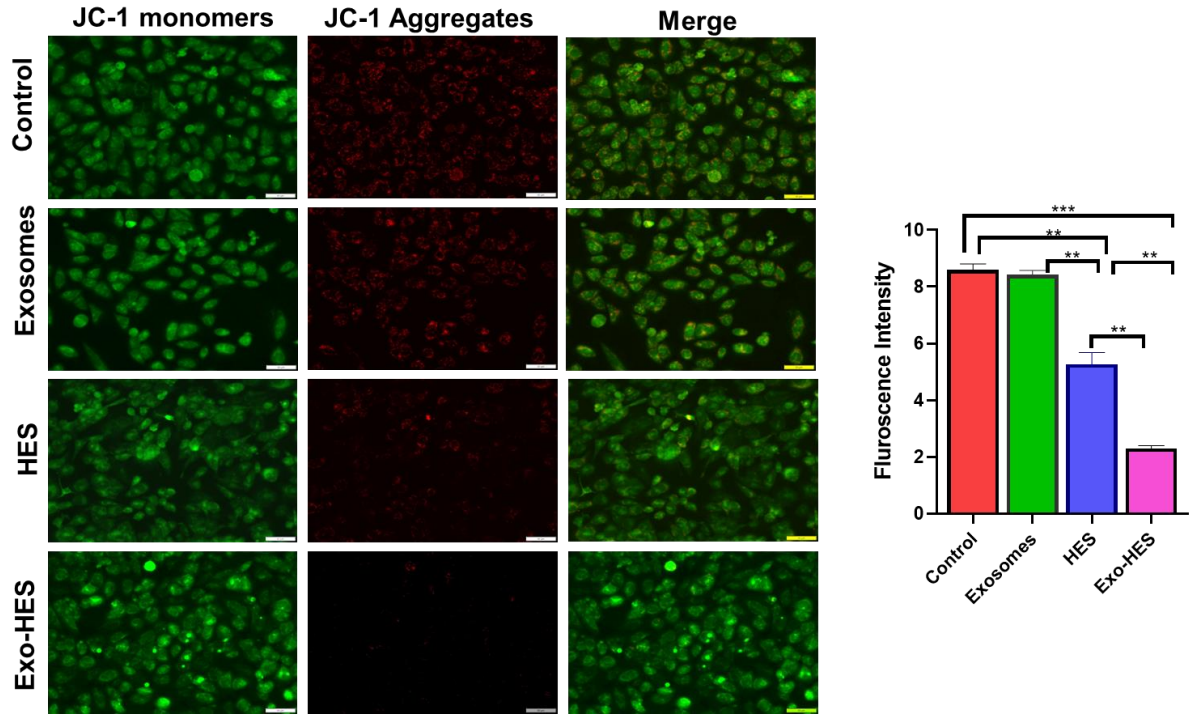

Figure 6.12 In the mitochondrial membrane potential assay, green fluorescence indicates JC-1 monomers and red fluorescence indicates the J-aggregates. Statistical analysis was performed by One-Way ANOVA followed by the Tukey P test with multiple comparisons and the significance level **$p < 0.01$, and ***$p < 0.001$.

6.4.10 Colony formation assay

The development of cell colonies, or cancer regrowth, is a critical aspect of cancer recurrence following chemotherapy or radiation treatment. The influence of drugs or formulated compounds on colony formation was evaluated through clonogenic assays. As depicted in Figure 6.13, the group treated with HES showed a significantly higher development of cell colonies ($p < 0.05$) compared to the cells treated with Exo-HES. These results suggest that the developed Exo-HES formulation may effectively prevent cancer recurrence.

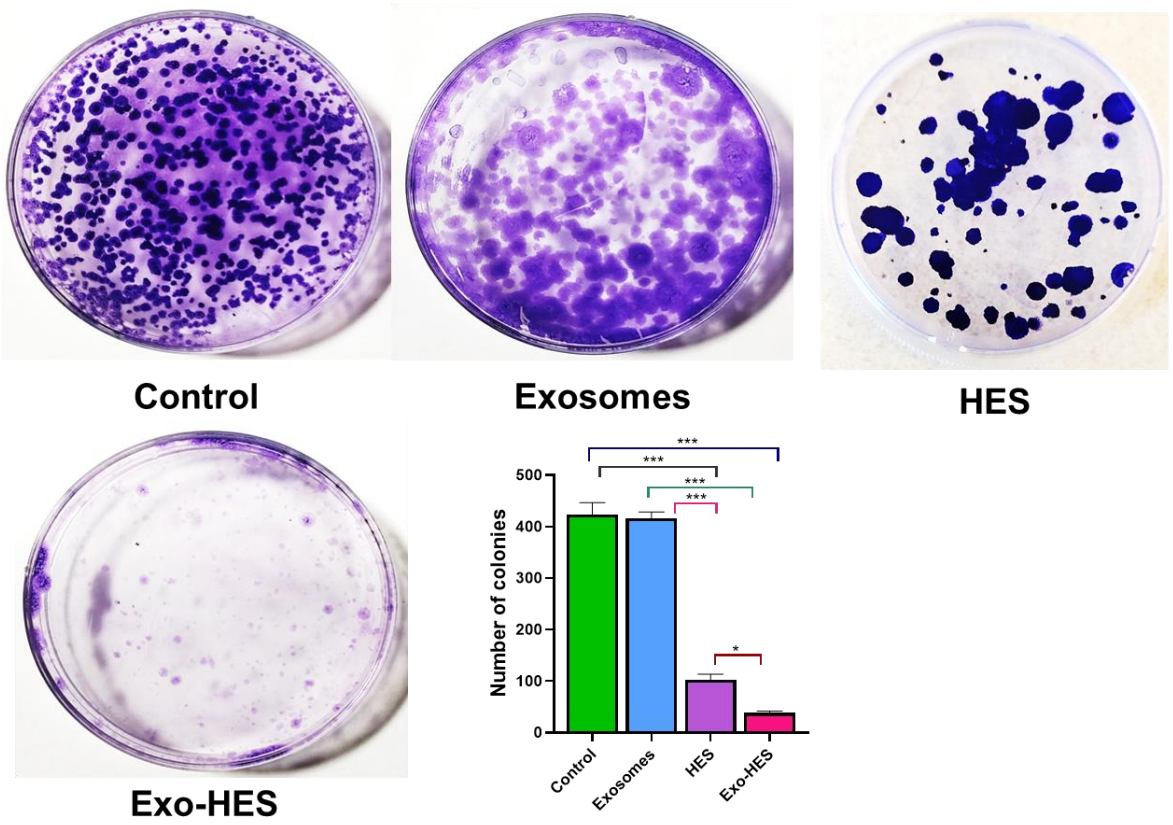

Figure 6.13 Colony formation assay was performed in B16F10 cell lines. Treatment was given with exosomes, HES, and Exo-HES. Statistical analysis was performed by One-Way ANOVA followed by the Tukey P test with multiple comparisons and the significance level $*p < 0.05$ and $***p < 0.001$.

6.4.11 Transwell migration assay

Melanoma, the most perilous form of skin cancer, poses a high risk of metastasis, primarily to the bone marrow and lungs. Metastasis in melanoma is driven by various factors, including inadequate oxygen and nutrients, evasion from immune cells, and the activation of specific metastatic factors. To investigate the potential of HES and Exo-HES in halting cell migration in melanoma, we conducted both a transwell migration experiment and a wound healing assay. In contrast to the higher HES concentration used in other *in vitro* efficacy studies (18 µM), a lower concentration of HES (10 µM) was employed in migration assays such as the transwell migration assay and wound healing assay. This reduction in HES concentration was based upon previous reports in which 18 µM concentration led to cell death and alterations in cell morphology. The results revealed that the migration of the control and HES-treated groups was

significantly higher than that of the Exo-HES-treated groups ($p < 0.05$), as illustrated in Figure 6.14. The inhibition of transwell migration observed could potentially be attributed to the suppression of the stromal cell-derived factor-1 (SDF-1)/ C-X-C chemokine receptor type-4 cascade mechanism [215]. Previous research has indicated the involvement of the SDF-1/CXCR-4 signaling pathway in activating tumor cell migration. Specifically, the phosphorylation cascade initiated by the SDF-1-activated CXCR-4 receptor, which is facilitated by HSP90 and leads to actin rearrangement, plays a role in cell migration [215]. Additionally, the ability of Exo-HES to inhibit MMP enzymes may also contribute to its capacity to hinder cell migration [216].

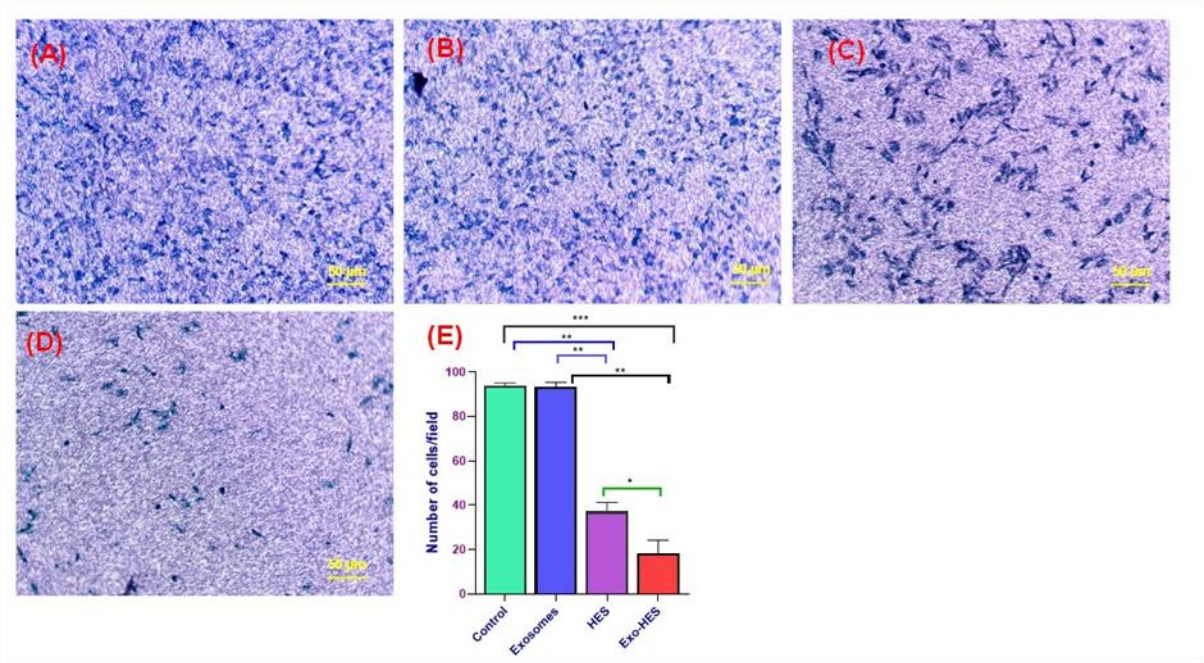

Figure 6.14 Transwell migration assay shows the Exo-HES significantly reduces the migration of B16F10 cell lines. (A) represents control, (B) treated with exosomes, (C) treated with HES, (D) treated with Exo-HES, (E) number of migrated cells/field calculated via microscope. Statistical analysis was performed by One-Way ANOVA followed by the Tukey P test with multiple comparisons and the level of significance *$p < 0.05$, **$p < 0.01$, and ***$p < 0.001$.

6.4.12 Wound healing assay

Similar to the transwell migration experiment, the wound healing assay was employed in B16F10 cell lines to further affirm the anti-metastatic properties of HES and Exo-HES. As

depicted in Figure 6.15, the wound healing process was markedly slower in the Exo-HES-treated cells compared to those treated with HES.

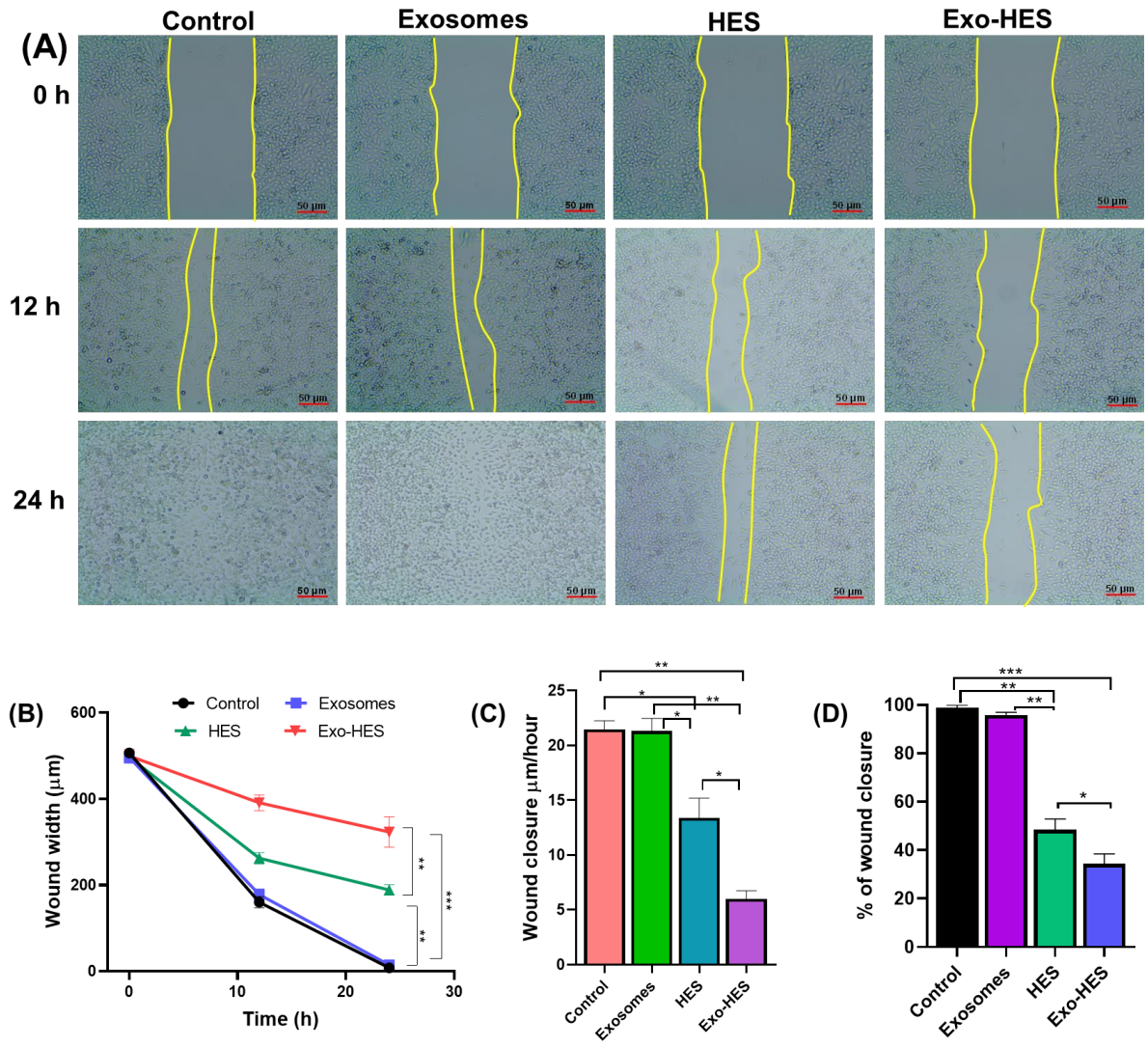

Figure 6.15 (A) Wound healing assay was performed in B16F10 cell lines, and healing was observed at 0 h, 12 h, and 24 h. The percent of wound healing is calculated via the (B-C) rate of the wound closure and (D) % of wound closure. Statistical analysis was performed by One-Way ANOVA followed by the Tukey P test with multiple comparisons and the level of significance *$p < 0.05$, **$p < 0.01$, and ***$p < 0.001$.

Additionally, the Exo-HES-treated cells exhibited a significantly lower wound closure percentage ($p < 0.001$) compared to the control and HES-treated cells (Figure 6.15B). Furthermore, the rate of wound closure per hour was notably reduced in Exo-HES. The combined results from the transwell migration assay and wound healing assay indicate that Exo-HES effectively suppresses cell growth and invasion, particularly by targeting

angiogenesis and metastasis pathways. The observed inhibition of cell migration may stem from a decrease in mast cell density, likely attributed to the suppression of Metallo matrix proteinase-9 (MMP-9), MMP-2, and MMP-8 production, along with a reduction in COX2 expression [217]. It's well documented that COX-2 and MMPs play crucial roles in angiogenesis, invasion, and metastasis, and our findings support this by demonstrating that HES can reduce the expression levels of MMP-2, MMP-9, and COX-2 [218, 219]. The *in vitro* data suggests that exosomes substantially enhance the anti-cancer efficacy of HES. However, further *in vivo* studies are imperative to validate its effectiveness.

6.4.13 Pharmacokinetics

Before proceeding to assess the effectiveness of HES when combined with exosomes in mice with tumors, it was essential to first evaluate the oral bioavailability of HES. This evaluation was carried out using SD rats. The data depicted in Figure 6.16 A and B illustrate the mean plasma concentration-time profiles following the oral administration of HES and Exo-HES. The results revealed that the plasma levels of HES were significantly elevated when delivered via Exo-HES compared to HES alone. One-way ANOVA and the Tukey P-test were used for statistical analysis. Significant differences were observed in the maximum concentration (Cmax) and the area under the curve (AUC) between free HES and Exo-HES. Specifically, the Cmax of HES from Exo-HES (2.740±0.105) was significantly higher, approximately 18.26-fold, than that of free HES (0.158±0.06), with a p-value <0.01. Moreover, the AUC0-t for Exo-HES (37.322±3.541) was found to be 37.6 times greater than that of free HES (0.929±0.021), indicating a significant increase with a p-value <0.001. Additionally, Exo-HES demonstrated a significantly prolonged Tmax of 10 h compared to 4 h for free HES, with a p-value <0.01. The improved bioavailability of HES can be credited to several factors: (i) decreased degradation of HES in the stomach, (ii) enhanced absorption of HES facilitated by exosomes, (iii) prolonged release of HES from exosomes, and (iv) enhanced systemic circulation of exosomes.

Additionally, the clearance rate observed for Exo-HES (0.708±0.004) was notably lower than that of HES alone (30.778±1.04), possibly due to the reabsorption of exosomes into the bloodstream during the filtration.

(A)

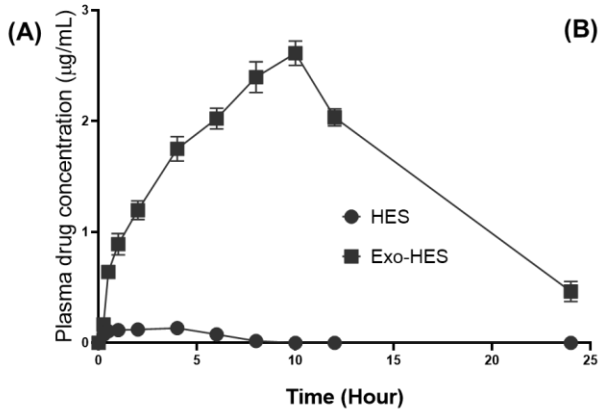

(B)

PK parameters	Unit	HES	Exo-HES
C_{max}	µg/mL	0.150± 0.06	2.740±0.105**
T_{max}	h	4	10**
AUC_{0-t}	µg/mL*h	0.411	36.322±3.541 ***
$AUC_{0-\infty}$	µg/mL*h	1.289±0.525	41.502±4.254
$t_{1/2}$	h	3.443 ± 0.261	6.411±0.382
K_e	1/h	0.201±0.002	0.108±0.004
MRT_{0-t}	h	4.150±0.182	10.148±1.145
$MRT_{0-\infty}$	h	6.463±0.541	13.031±0.254
Vz/F	(mg/kg)/(µg/mL)	13.802±0.306	4.457±0.244
CL/F	(mg/kg)/(µg/mL)/h	2.778±0.104	0.481±0.003

Figure 6.16 Pharmacokinetic profile of HES and Exo-HES after oral administration at 25 mg/kg. (A-B) represents the pharmacokinetic profile and pharmacokinetic parameters in tabular form. Statistical analysis was performed by One-Way ANOVA followed by the Tukey P test with multiple comparisons and the level of significance $**p < 0.01$ and $***p < 0.001$. Values are represented as mean±SD.

Abbreviations

Cmax peak plasma concentration, Tmax time to reach peak plasma concentration, AUC0-t area under the plasma drug concentration-time curve from time 0 to 24 h, AUC0-∞ area under the plasma drug concentration-time curve from time 0 to infinity h, t1/2 elimination half-life, Ke elimination rate constant, MRT0-t mean residence time from time 0–24 h, MRT0-∞ mean residence time from time 0 to infinity h, Vz/F apparent volume of distribution, CL/F apparent systemic clearance following an oral administration.

6.4.14 Anti-cancer efficacy study

Swiss mice with B16F10-induced melanoma were used to investigate the anticancer efficacy of HES-loaded exosomes. The melanoma was induced in Swiss mice using well-established procedures [220], involving the subcutaneous implantation of $5x10^5$ B16F10 cells to generate tumors. Once the tumors reached a size of 60–80 mm^3, the animals were randomized into various groups, and treatment commenced on the eighth day, continuing until the 20^{th} day. The treatments included DTIC at 5 mg/kg by intraperitoneal injection, and HES equivalent to 50 mg/kg administered orally. Tumor evaluation was based on parameters such as tumor weight, tumor growth inhibition (TGI), final tumor volume, and tumor volume doubling time.

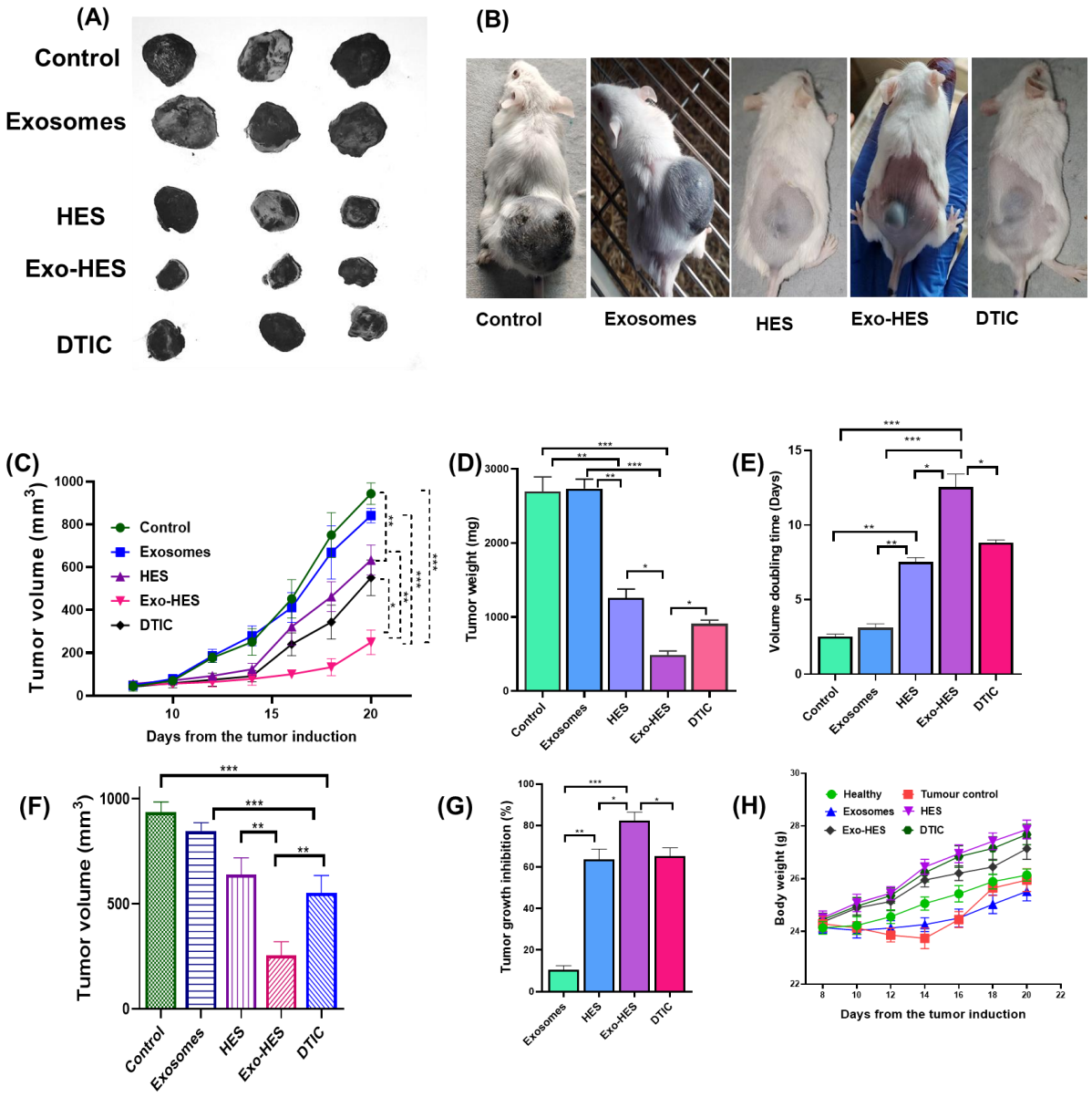

Figure 6.17 Tumor images and tumor volumes of control, Exo, HES, Exo-HES, and DTIC-treated groups. (A) Final day tumors, (B) represents final-day tumors, (C) Tumor regression analysis representing the tumor volume in different treatment groups with respect to time, (D) Tumor weight, (E) tumor volume doubling time, (F) final tumor volume, (G) percent tumor growth inhibition, and (H) Body weight. Statistical analysis was performed by One-Way ANOVA followed by the Tukey P test with multiple comparisons and the level of significance *$p < 0.05$, **$p < 0.01$, and ***$p < 0.001$.

Following the treatment period, the average tumor growth inhibition was determined, showing values of 65.28, 25.3, 82.37, and 10.54% for the DTIC, HES, Exo-HES, and exosomes groups, respectively (Figure 6.17 E). The average final tumor sizes were observed as 910, 820, 625, 244, and 510 mm^3 for the control, exosomes, HES, Exo-HES, and DTIC groups, respectively

(Figure 6.17 A and D). The average tumor weights were found to be 2696.66±16048, 2733.33±105.21, 2215.66±97.40, 488.33±42.88, and 909.33±39.54 mg for the control, exosomes, HES, Exo-HES, and DTIC groups, respectively (Figure 6.17 B). Additionally, the average tumor volume doubling time was calculated as 2.52±0.13, 3.11±0.20, 7.54±0.22, 12.56±0.69, and 8.82±0.14 days for the control, exosomes, HES, Exo-HES, and DTIC groups, respectively (Figure 6.17 C). The results indicated that Exo-HES exhibited significantly higher anticancer efficacy than free HES ($p<0.01$). The improved anti-tumor effectiveness of HES can be attributed to increased bioavailability, reduced clearance, enhanced Cmax, and Tmax.

6.4.15 Histopathology

Histopathological analysis of essential organs (heart, lung, liver, kidney, and spleen) from treated mice was conducted to further evaluate the potential toxicity of Exo, HES, Exo-HES, and DTIC. The organs were removed and stained with H&E dye. The results revealed normal histological features for the hepatocytes and portal vein in the healthy, tumor control, exosomes-treated, HES-treated, and Exo-HES-treated groups, as illustrated in Figure 6.18. However, the group treated with DTIC exhibited a ruptured portal vein configuration, possibly indicating damage to sinusoidal endothelial cells, leading to their death and extrusion into sinusoids with subsequent obstruction [221]. Aside from this observation of hepatotoxicity in the DTIC-treated group, no harmful effects or alterations were noted in the kidneys (nephron structures), heart, spleen, or lungs (pulmonary fibrosis). The overall findings from the histopathological analysis suggest that exosomes, HES, and Exo-HES demonstrate safety profiles, with no apparent toxicity in the examined organs.

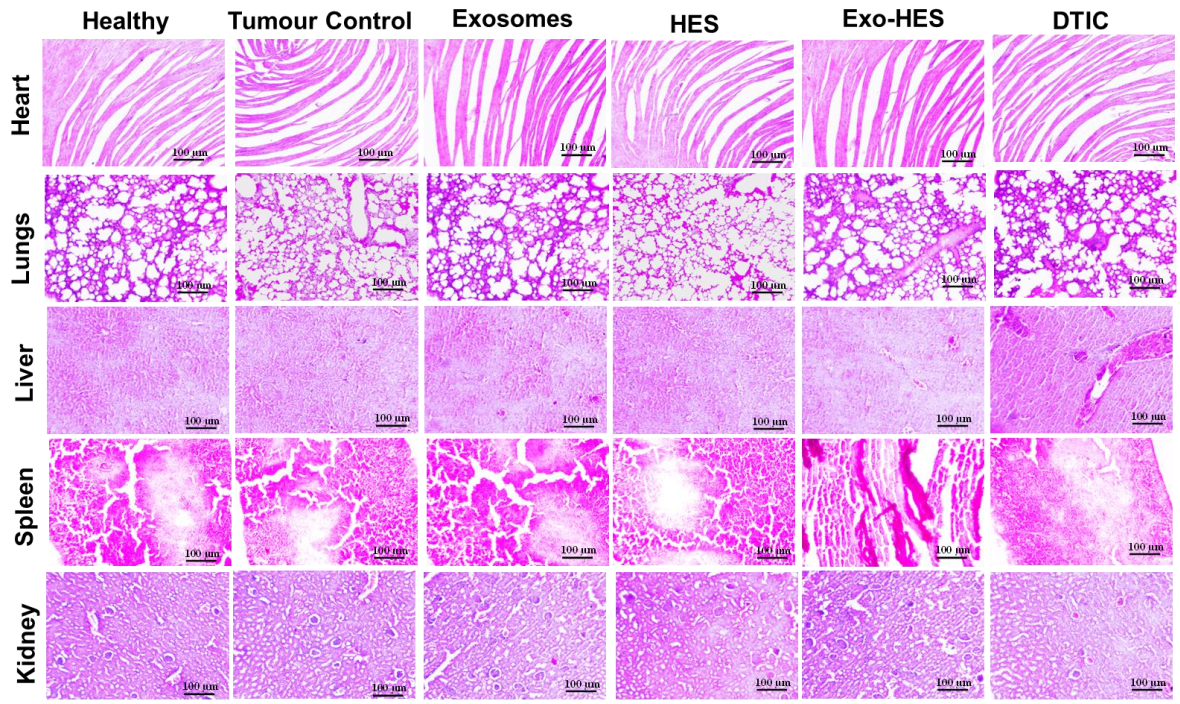

Figure 6.18 Histopathology of different vital organs was performed by H&E staining. Organs were isolated from tumor-bearing mice after the treatment.

6.4.16 Biochemical assay

Biocompatibility is a critical consideration for drug delivery systems and anticancer substances, with the potential systemic or tissue toxicity being a primary concern. To assess the compatibility of drugs and delivery vehicles, it is essential to evaluate biochemical markers that indicate systemic cytotoxicity after the completion of treatment. In this study, various biochemical parameters, including ALT, AST, and others, were measured to assess potential systemic cytotoxicity. As depicted in Figure 6.19, all biochemical parameters remained within the normal range in all groups, except for the DTIC-treated group. In this group, levels of ALT, AST, urea, ALP, and creatinine were significantly elevated compared to all other groups. The increased levels of ALT, AST, and ALP may indicate liver toxicity, while the increased levels of urea and creatinine may suggest kidney toxicity. However, it's noteworthy that kidney toxicity was not observed in the histopathological analysis. These findings highlight the importance of assessing both biochemical markers and histopathology to comprehensively evaluate the safety and biocompatibility of drug delivery systems and anticancer agents.

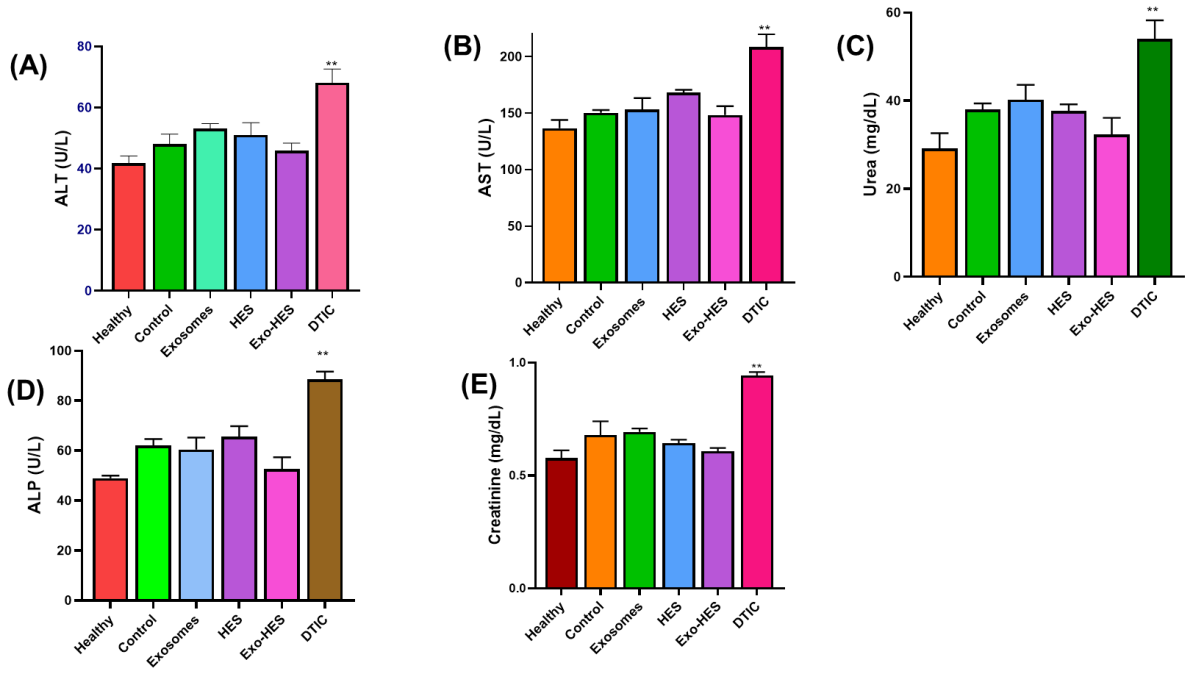

Figure 6.19 Assessment of biochemical parameters in plasma after treatment, including (A) ALT, (B) AST, (C) ALP, (D) Urea, and (E) Creatinine. Statistical analysis was conducted using One-Way ANOVA followed by the Tukey P test with multiple comparisons. The significance levels are indicated as $^{**}p < 0.01$.

6.5 Conclusion

This study aimed to enhance the half-life and therapeutic efficacy of HES-loaded exosomes in both *in vitro* and *in vivo* settings. Exosomes were isolated from bovine milk, and HES was loaded into exosomes through sonication. Characterization revealed that the biological particles are spherical with a particle size around 100 nm. *In vitro* studies, including cytotoxicity, DNA fragmentation, ROS mitochondrial membrane assay in B16F10 cell lines, and *in vivo* studies such as pharmacokinetics and B16F10-induced melanoma in a Swiss mice model, confirmed the improved efficacy of HES upon loading into exosomes. Toxicity and histopathology studies further confirmed the safety of the developed formulation strategy. These findings collectively suggest that exosomes loaded with HES represent a promising nanocarrier strategy to enhance the therapeutic effectiveness of hesperidin in melanoma treatment. The presented approach holds the potential for addressing the current limitations in melanoma therapy and provides a foundation for future research and clinical applications.

However, further *in vivo* investigations employing RT-PCR or western blotting methods are necessary to validate the HES mechanism.

6.6 Summary points

- HES has shown its treatment potential against melanoma
- Due to the poor water solubility and low oral bioavailability, bovine milk-derived exosomes were used to deliver the HES.
- DLS results reveal that exosomes were below 150 nm, and HR-SEM and AFM confirmed the spherical shape of exosomes.
- Exo-HES formulation showed improved dose-dependent cytotoxicity against B16F10 cells compared to free HES solution and showed no cytotoxicity towards the noncancerous healthy HEK 293 cell line, reflecting selective cytotoxicity to the cancerous cell.
- Exo-HES formulation showed improved *in vitro* efficacy compared to free DHA confirmed by various *in vitro* assays.
- The oral bioavailability of HES significantly improved when loaded into exosomes compared to free HES.
- The results of the tumor regression study in the syngeneic transplantation melanoma model (in Swiss female mice) revealed improved therapeutic activity of Exo-HES compared to free HES.
- Exo-HES formulations significantly reduced the migration.
- The overall result revealed that exosomes are a suitable vehicle for delivering HES in the treatment of melanoma.